國立臺灣大學生命科學院植物科學研究所

碩士論文

Institute of Plant Biology

College of Life Science

National Taiwan University

Master Thesis

BABA 誘發免疫反應對抗細菌性病原菌之作用機制

Dissecting out the Role of β-Aminobutyric Acid in Plant Immunity against Bacterial Pathogen *Pst* DC3000

研究生：朱柏威

Student: Po-Wei Chu

指導教授：金洛仁博士

Advisor: Laurent Zimmerli, Ph.D.

中華民國 99 年 10 月

October, 2010

國立臺灣大學碩士學位論文
口試委員會審定書

BABA 誘發免疫反應對抗細菌性病原菌之作用機制

Dissecting out the Role of β-Aminobutyric Acid in Plant Immunity against Bacterial Pathogen *Pst* DC3000

本論文係朱柏威君(R97B42019)在國立台灣大學植物科學研究所完成之碩士學位論文，於民國 99 年 10 月 20 日承下列考試委員審查通過及口試及格，特此證明

口試委員:

台灣大學植物科學研究所　助理教授

金洛仁　博士　Dr. Laurent Zimmerli

台灣大學植物科學研究所　副教授

吳克強　博士

台灣大學農業化學研究所　助理教授

林乃君　博士

誌謝

我曾經參加過許多學長姐的論文口試。那等待最終宣判的時刻，總是全程的最高潮。一旦門後的會議結束，學生的命運隨即抵定。踏進教室聆聽結果的這段路途，既漫長而又沉重。我總好奇裡頭等待學長姐的究竟為何？這是局外人無法窺探的秘密。如今，我終於親自踏上這條征途，為兩年的研究旅程畫上句點。

這兩年，充滿著扎實的研究與學習，指導教授 Dr. Laurent Zimmerli 著實功不可沒。在 Dr. Zimmerli 引領下，我踏出植物分子生物學的第一步；他並且教導，如何令我每個步伐走得嚴謹而穩健。我體認到科學研究是門重視邏輯與思考的藝術，而非任意拼湊無數實驗的雜燴料理。我的論文嘗試集合兩年的研究成果，並透過嚴謹的論述，將其鋪陳為一篇具啟發性的「故事」。也感謝兩位口試委員，吳克強老師與林乃君老師，百忙中抽空協助修改文章，使論文更臻完美。

研究的路途必然有許多挫折，面對這些困境，多虧可愛的實驗室成員們願意傾聽與給予鼓勵，讓我在數不盡的實驗死巷裡重燃希望。尤要感謝敬偉學長、Terry 學長，我們曾經組成默契絕佳的敢死隊，一起篩選過無數的突變株。沒有這段苦辛，必然沒有今日的 LRR-PK 小組(笑)。在敬偉學長、小喬與佳楠的共同協助下，我們一起令 LRR-PK 小組茁壯成長。同時感謝實驗室的博士後研究員，Dominique，他熱心地指導我完成研究生涯的第一個基因轉殖阿拉伯芥。吳老師實驗室的峻惟學長與芳芳，提供許多實驗技術的協助，令我感念不已。這些共同奮鬥的戰友們，都是促成這篇論文的無名英雄。

兩年來，我將不少夜晚與假日的休息、陪伴親友的寶貴時間，奉獻於實驗中。為此我想向遠在台中的父母親與女友，豆豆，致上無比歉意。進入研究所後，返鄉的次數明顯減少許多。對於不明瞭孩子遠在異鄉為何而忙的雙親而言，這必是

一種難熬的等待。同時我非常感激豆豆，總是義無反顧的陪伴在我身邊，一起分享無數喜樂與哀愁。

兩年，對於研究工作而言實不算長，我僅能淺嚐「科學」這道佳餚。然而，我從其中認識了鑽研任何課題應該掌握的要旨與不輕言放棄的態度。因此無論人生下一階段為何，我相信必能秉持這兩年所學，並全力以赴。

謹以此論文，獻給所有關心我的師長、家人、同學與朋友們。

朱柏威　謹誌於台中家中

2010/10/25

摘要

BABA (beta-aminobutyric acid)是一種無法用於合成蛋白質的胺基酸，但是卻被發現能有效促進植物對病原菌的抵抗性。植物經 BABA 處理後，一旦感懶細菌性斑點病病原菌 (*Pseudomonas syringae* pv. *tomato* DC3000, *Pst* DC3000)，水楊酸 (salicylic acid, SA) 訊息傳導途徑中的 *PR1* 基因將被快速誘發而表現。本論文報導由 BABA 所引起的病原菌抵抗性，並非完全依賴於水楊酸訊息傳導途徑；BABA 能誘發植物的早期免疫反應 (plant early defense response)。一經細菌 *Pst* DC3000 感染，BABA 誘發諸多免疫基因表現，且這些基因分別隸屬於不同訊息傳導途徑，例如，MAPK (mitogen-activated protein kinases) ，乙烯 (ethylene, ET)，以及其他訊息途徑。同時，BABA 能有效誘發細菌感染時所引起的胝質累積 (callose deposition)。除此之外，如將水楊酸的突變株 *sid2* 以 RNA 干擾技術(RNA interference)造成 *PR2* 基因靜默(gene silencing)，不會改變 BABA 對該突變株的作用，顯示 *PR2* 的存在與否對於 BABA 的作用沒有影響。為深入瞭解 BABA 如何調節阿拉伯芥的免疫作用，金洛仁博士的實驗室成員們測試七十餘株突變株對於 BABA 的敏感性與細菌 *Pst* DC3000 的感病性。本論文發現某一 LRR 家族蛋白激酶 (leucine-rich repeat protein kinase, LRR-PK)的突變株，不僅易受細菌感染、胝質的累積量減少，且對於 BABA 的敏感度降低。該 LRR-PK 表現於細胞膜。且於植物遭受細菌感染，或者感受到病原相關分子模式(pathogen-associated molecular patterns, PAMPs)時，*LRR-PK* 基因能被快速誘導表現。初步證據顯示此基因參與阿拉伯芥早期的免疫反應。除此之外，本研究亦發現四磷酸雙腺苷水解酶(Ap_4A hydrolase)對於阿拉伯芥抵抗腐生性病原菌(necrotrophic pathogen)具有重要功能。該基因的突變株對於真菌性灰黴病病原菌(*Botrytis cinerea*)和細菌性軟

腐病病原菌(*Erwinia carotovora* subsp. *carotovora*)較為感病。

關鍵字：BABA、阿拉伯芥、細菌性斑點病菌、水楊酸、植物早期免疫反應、胝質累積、蛋白激酶、四磷酸雙腺苷水解酶

Abstract

The non-protein amino acid beta-aminobutyric acid (BABA)has been known for years to be an effective inducer of resistance against pathogen infection. When BABA-pretreated Arabidopsis plants are challenged with the pathogenic bacteria *Pseudomonas syringae* pv. *tomato* DC3000 (*Pst* DC3000), a strong potentiation of *PR1* expression is observed. *PR1* is the marker gene for salicylic acid (SA)-related defense response. Here, we report that BABA-mediated bacterial resistance acts in a partly SA-independent manner to prime the early Arabidopsis defense response. Upon *Pst* DC3000 infection, mitogen-activated protein kinase (MAPK) cascade genes, ethylene (ET) and other signaling pathways were potentiated by BABA pretreatment in both Col-0 wild type and in the SA biosynthetic *sid2* mutant. Callose deposition in response to *Pst* DC3000 inoculation was also primed by BABA. In addition, RNAi-mediated *PR2* gene silencing in *sid2* mutant demonstrated BABA-induced resistance (BABA-IR) to *Pst* DC3000 similar to *sid2* indicating that *PR2* is not critical for BABA-induced resistance in *sid2.*

To further investigate how BABA regulates Arabidopsis immunity, members of Zimmerli's laboratory tested over 70 T-DNA knock-out mutant lines for their sensitivity towards BABA and *Pst* DC3000 infection. Two T-DNA knock-out lines of a leucine-rich repeat protein kinase (LRR-PK) demonstrated enhanced bacterial susceptibility, reduced callose deposition, as well as impaired BABA sensitivity. This LRR-PK localizes to the plasma membrane. Upon *Pst* DC3000 infection and PAMPs treatment, this *LRR-PK* gene was rapidly induced. Hence, our preliminary data

suggest that this gene is involved in Arabidopsis early defense responses. In addition, one gene was found important for plant resistance to necrotrophic pathogens. Mutation of *AtNUDX25*, one Ap_4A hydrolase, led to enhanced susceptibility to *Botrytis cinerea* and *Erwinia carotovora* subsp. *carotovora* strain WPP14 (*Ecc* WPP14).

Key words: BABA, Arabidopsis, *Pseudomonas syringae*, SA, early defense response, callose deposition, leucine-rich repeat protein kinase, Ap_4A hydrolase

List of Figures

List of Tables

Abbreviations

BABA	β-aminobutyric acid
***Pst* DC3000**	*Pseudomonas syringae* pv. *tomato* DC3000
Pst* DC3000 *hrcC	*Pseudomonas syringae* pv. *tomato* DC3000 *hrcC*⁻
PAMP	pathogen-associated molecular pattern
PTI	PAMP-triggered immunity
SA	salicylic acid
JA	jasmonic acid
ET	ethylene
PR1	*PATHOGENESIS-RELATED 1*
PR2	*PATHOGENESIS-RELATED 2*
SID2	*SALICYLIC ACID INDUCTION DEFICIENT 2*
NPR1	*NONEXPRESSOR OF PR GENES 1*
PDF1.2	*PLANT-DEFENSIN 1.2*
FLS2	FLAGELLIN SENSITIVE 2
BAK1	BRI1-ASSOCIATED RECEPTOR KINASE 1
FRK1	FLG22-INDUCED RECEPTOR-LIKE KINASE 1
CBP60g	CAM-BINDING PROTEIN 60-LIKE G
LRR-PK	leucine-rich repeat protein kinase

Contents

Introduction

PAMP-Triggered Immunity against Bacteria: Pattern Recognition Receptors

Pathogen perception and quick induction of defense response is important during plant innate immunity. This form of immune response is mediated by a group of membrane proteins termed “pattern recognition receptors” (PRRs), which recognize highly conserved molecular signatures characteristic of whole class of microbes defined as “pathogen-associated (or microbe-associated) molecular patterns” (PAMPs or MAMPs). Perception of PAMPs by PRRs leads to a chain of signaling events in plants, which is called PAMP-triggered immunity (PTI) (Boller and Felix, 2009; Nicaise et al., 2009).

One well studied PAMP is flagellin, the protein component of bacterial motility organ flagellum. Flg22, a synthetic 22-amino-acid polypeptide that corresponds to a highly conserved region of eubacterial flagellin, elicits responses in most plant species and acts as potent elicitors at subnanomolar concentrations (Felix et al., 1999).

Flg22 treatment leads to strong growth inhibition in young seedling. This was used in a mutant screen, yielding a number of mutants that were insensitive to flg22. One of the mutated loci, *FLAGELLIN-SENSING2* (*FLS2*) was found to encode a LRR receptor-like kinase (LRR-RLK) and later proved to be the PRR for flg22 (Gómez-Gómez and Boller, 2000; Chinchilla et al., 2006).

Besides flg22, the elongation factor Tu (EF-Tu) acts as a very potent bacterial PAMP in Arabidopsis as well (Kunze et al., 2004). EF-Tu is one of the most abundant and most conserved proteins in bacteria. Peptides corresponding to the acetylated N

terminus of EF-Tu, called elf18 and elf26, triggered PAMP responses in Arabidopsis also in subnanomolar concentrations. Although EF-Tu is mostly intracellular, its release from lysis of dying bacteria during plant colonization should be sufficient to trigger its subnanomolar recognition (Zipfel et al., 2006).

A targeted reverse-genetic approach was used to identify a receptor kinase essential for EF-Tu perception. The T-DNA insertion mutant *efr* was completely insensitive to elf18/elf26, although still responded normally to flg22. *Nicotiana benthamiana*, a plant unable to perceive EF-Tu, acquires EF-Tu responsiveness upon transient expression of *EFR* (Zipfel et al., 2006). These findings directly demonstrated that EFR is the PRR for EF-Tu (Zipfel et al., 2006).

FLS2 and EFR protein structures resemble each other, and are both classified into the family of leucine-rich repeat receptor-like kinases (LRR-RLKs). The Arabidopsis genome encodes more than 200 LRR-RLKs. FLS and EFR both belong to the subfamily LRR XII. FLS2 contains an extracellular domain of 28 LRR motifs, while EFR has 21 LRRs. LRR motifs are known from crystallographic studies to form a highly ordered horseshoe-like solenoid structure (Boller and Felix, 2009). Site-directed mutational analysis and other approached were conducted to investigate how LRRs contribute to flagellin perception. The LRRs 9 to15 was identified important for flg22 binding, but the actual binding site remains unknown (Chinchilla et al., 2006; Dunning et al., 2007; Robatzek et al., 2007). Similar to FLS2, the exact elf18 binding site is still unknown in EFR.

Interestingly, recent study has shown that FLS2 interacts with another LRR-RLK, BAK1 (BRI1-associated receptor kinase 1), immediately (less than 2 min) after

treatment of ligand flg22 (Chinchilla et al., 2007). *bak1* mutant still exhibits normal binding to flg22, but its early and late flg22 induced responses are strongly impaired. Besides, *bak1* mutant shows reduction in early elf18-triggered response of ROS production (Chinchilla et al., 2007). Thus, BAK1 is an important PTI regulator that acts concomitantly with PRRs.

Although BAK1 belongs to LRR II family, it contains only 4 LRR motifs in its extracellular domain. It is suggested that receptor dimerization between BAK1 and FLS2 may play essential role in flagellin signaling. The current model of FLS2 and BAK1 is that, upon binding of flg22, the LRR domain of FLS2 changes conformation, allowing it to heterodimerize with BAK1 to form a tight complex. Interaction of the ectodomains of FLS2 and BAK1 also brings the intracellular kinase domains into contact, thus allowing initiation of intracellular signaling, likely by transphosphorylation events (Boller and Felix, 2009).

PAMP-Triggered Immunity against Bacteria: Downstream Signaling

In Arabidopsis, PAMPs induced responses, including early responses like ion fluxes, oxidative burst, activation of MAPK cascade, calcium-dependent protein kinases (CDPKs) cascade, ethylene biosynthesis and late responses like callose deposition (Boller and Felix, 2009; Boudsocq et al., 2010).

MAPK networks are involved in various processes in eukaryote cells, including plant defense. Activation of MAPK cascade leads to activation of WRKY-type transcription factors, key regulators of plant defenses (Eulgem and Somssich, 2007). Following activation of WRKYs, FRK1 (FLG22-INDUCED RECEPTOR-LIKE

KINASE 1), one MAPK-specific target LRR-RLK, is rapidly induced to turn on downstream signaling (Asai et al., 2002).

Ca^{2+} influx is another PAMP triggered early response. It was recently shown that CDPKs play important roles as Ca^{2+} sensors in flg22 or MAMP signaling, and were quickly activated following flg22 elicitation (Boudsocq et al., 2010). Unexpectedly, CDPKs and MAPK cascades act differentially in PAMP-mediated regulatory programs to control early genes involved in the synthesis of defense peptides and metabolites, cell wall modifications and redox signaling (Boudsocq et al., 2010).

PAMPs also induce rapid and transient production of ROS in an oxidative burst. Reactive oxygen species can act as antibiotic agents directly, as well established in macrophages in animals, or they may contribute indirectly to defense by causing cell wall cross-linking; in addition, reactive oxygen species may act as secondary stress signals to induce various defense responses (Apel and Hirt, 2004). However, the relative position of oxidative burst in the sequence of signaling events during PTI is still unclear (Nicaise et al., 2009).

The accumulation of callose, a β-1, 3-glucan polymer, between the cell wall and the plasma membrane is a classical marker of PTI after bacterial infection or PAMPs perception (Gómez-Gómez et al., 1999), although the biological foundation of this response is still unclear.

Stomatal closure is part of a plant innate immune response to restrict bacterial invasion. PAMPs treatment also induce stomatal closure (Melotto et al., 2006). Stomatal guard cells perception of bacteria requires FLS2 receptor, and

guard-cell-specific OST1 kinase (Melotto et al., 2006).

The Nudix-motif Containing Protein Family

In plant, one group of proteins has recently drawn much attention due to its involvement in disease resistance. This protein family, Nudix hydrolase protein family, has been identified for a long time with few understandings on their physiological functions.

The Nudix hydrolase protein family contains the enzyme activity of hydrolyzing nucleotide derivatives (also called **nu**cleoside **di**phosphates linked to some moiety **X**, hence the acronym "Nudix"). They usually catalyze cleavage of a diphosphate (PP_i) bond, thus permitting nucleotide moieties to be recycled.

This family is characterized by a conserved Nudix motif, $GX_5EX_7REVXEEXGU$, where U represents a bulky hydrophobic amino acid such as Ile, Leu, or Val and X is any amino acid (Ogawa et al., 2008). Although Nudix motif is common to all of these proteins, they actually act upon a wide range of substrates, including nucleotide sugars (e.g. ADP-ribose), (d)NTPs, nicotinamide nucleotides (e.g. NADH), dinucleoside polyphosphates (e.g. Ap_nA; n= 3-6), CoA, and mRNA caps. Therefore, Nudix hydrolases can be further divided into subfamilies according to their substrate specificities.

In Arabidopsis, at least 27 genes encoding Nudix hydrolase homologues have been identified (Ogawa et al., 2008). Two of them were already found to play important role in plant resistance against certain stresses (Ogawa et al., 2005; Ge et al., 2007).

AtNUDX1 is a functional homologue of *E. coli* MutT in Arabidopsis, its expression in *E. coli mutT*⁻ strain highly reduced the frequency of spontaneous mutations in bacteria (Ogawa et al., 2005). AtNUDX1 protein has the ability to hydrolyze 8-oxo-dGTP, a mutagenic nucleotide, and thus plays an important role in protection against oxidative DNA and RNA damage in plant cells.

AtNUDX7 catalyzes the hydrolysis of NADH. It was first identified as a stress-induced gene, and the knock-out mutant was highly resistant to bacterial pathogen, *Pst* DC3000 (Jambunathan and Mahalingam, 2006). One study pointed out that *atnudx7* mutation leads to perturbation of cellular redox homeostasis and a higher level of NADH in pathogen-challenged leaves. They also hypothesized, this alteration of cellular antioxidant status might "prime" the cells for the amplified defense response. In general, AtNUDX7 functions as a negative regulator of basal immunity in Arabidopsis.

On the other hand, another group of AtNUDXs, Nudix Ap_4A hydrolase (hereafter referred to as Ap_4Aase), is less known about their physiological functions.

Ap_4Aase from the narrow leafed blue lupine, *Lupinus angustifolius*, has been well studied on the mechanism of enzymatic catalysis (Guranowski et al., 1994). Three putative Ap_4Aases in Arabidopsis showing high identity with lupine enzyme are designated as AtNUDX25, AtNUDX26, and AtNUDX27 respectively. Among them, AtNUDX25 was shown to efficiently hydrolyze Ap_4A asymmetrically into ATP and AMP (Szurmak B, 2008), while AtNUDX26 and -27 preferentially hydrolyzed Ap_4A or Ap_5A (Ogawa et al., 2008). AtNUDX25 also differed from AtNUDX26 and -27 in subcellular localization.

The enzyme substrate, Ap_4A, is found in organisms from Archeae to humans and is predominantly a by-product of protein synthesis, specifically by aminoacyl-RNA synthetases (Goerlich et al., 1982). So far, the biological significance of Ap_4A is not fully understood. In prokaryote, *Salmonella typhimurium*, Ap_4A accumulates under condition of oxidation and heat-shock stress, and is thus described as "alarmones" (Lee et al., 1983). In human cell cultures, regulation of Ap_3A/Ap_4A ratio was suggested to be involved in cell differentiation and apoptosis (Vartanian et al., 1997). One recent study on animal mast cell showed that, upon immunological challenge by IgE-antigen complex, Ap_4A level elevated in a MAPK-dependent fashion. This accumulation leads to dissociation of the transcription factor, and caused downstream gene activation (Yannay-Cohen et al., 2009).

Induced Resistance and Priming with the SAR Inducer, BTH

Besides the essential and well studied PAMP-triggered immunity, plants also possess inducible defense responses against pathogen attack. Upon infection by pathogen, plant develops enhanced resistance to subsequent infections by a broad spectrum of pathogens, either in the area of primary infection or in the distal, uninfected organs (Durrant and Dong, 2004).

The mechanism of induced resistance is usually linked with the ability of plants to induce cellular defense responses more rapidly and to a stronger degree in response to a much lower level of stimulus, either pathogen infection or abiotic stresses (Kohler et al., 2002). This phenomenon is also termed as "priming".

Although the priming has been known for years as a crucial part of induced

resistance, the molecular mechanisms and genetic basis of priming remained largely unclear.

One well studied type of induced resistance (IR) is systemic acquired resistance (SAR), which requires the signal molecule salicylic acid (SA) and is associated with accumulation of pathogenesis-related (PR) proteins (Durrant and Dong, 2004). SAR can also be induced by exogenous application of SA or its synthetic analogs, 2,6-dichloroisonicotinic acid (INA) and benzothiadiazole (BTH) (Kohler et al., 2002). In recent years, SAR and its potent inducer, BTH, were largely used for investigating mechanisms of cell priming.

As mentioned, a strong *PR1* gene activation was observed in BTH-pretreated plants. Besides, BTH pretreatment also greatly augmented the *PHENYLALANINE AMMONIA-LYASE* (PAL) gene expression and callose deposition following subsequent *Pst* DC3000 infection, wounding with forceps, or infiltration of water into leaves (Kohler et al., 2002). PAL is a key enzyme in the phenylpropanoid pathway that leads to a variety of defense-related plant secondary metabolites such as SA, phytoalexins, and lignin-like polymers (Hahlbrock and Scheel, 1989).

Furthermore, a recent publication revealed the involvement of MAPK cascade in the process of priming (Beckers et al., 2009). Using BTH as inducer, *MPK3* and *MPK6* transcripts and inactive proteins accumulated within 72 h. BTH-pretreated plants showed enhanced activation of kinases activity in response to subsequent virulent *Psm* ES4326 infection. In *mpk3* and *mpk6* mutant, BTH-mediated priming for enhanced *PAL* and *PR1* gene expression was highly attenuated (Beckers et al., 2009).

However, the BTH potentiation of PAL gene expression, callose deposition and

MPK3 and MPK6 activation were all absent in Arabidopsis *non-expressor of PR genes 1* (*npr1*) mutant. NPR1 is a positive regulatory protein which induces defense gene expression and activating SAR in response of SA (Beckers et al., 2009).

Induced Resistance and Priming with BABA

Other than SA and BTH, one distinct chemical compound called β-aminobutyric acid (BABA) was also reported to be an effective inducer of resistance to bacterial pathogens (Zimmerli et al., 2000), fungal pathogens (Zimmerli et al., 2001; Flors et al., 2008), insects, and abiotic stresses like drought, salt and heat (Jakab et al., 2005; Zimmerli et al., 2008). Interestingly, BABA is a synthetic non-protein amino acid, which does not resemble any biologically active molecule in plants, except for some amino acids.

Research on the mechanism of BABA-induced resistance (BABA-IR) in Arabidopsis has shown that it is mostly based on priming for different stress-inducible defense responses. In the case of bacterial pathogen *Pst* DC3000, although BABA pretreatment does not directly induce expression of *PR1* (which was induced in the case of BTH), *PR1* gene expression was strongly potentiated in BABA-IR against bacteria (Zimmerli et al., 2000). Hence, the signaling pathway controlling BABA-IR is partially different from that of SAR.

However, BABA was found inactive in *npr1* mutant and transgenic NahG plants. NahG transgenic plants overexpressing a salicylate hydroxylase gene (*NahG*) have low levels of SA and are unable to undergo SAR. Hence, BABA-IR against the bacteria *Pst* DC3000 resembles SAR in that it requires endogenous accumulation of

SA (Zimmerli et al., 2000).

On the other hand, it seems that BABA-IR to other pathogens depends on signaling pathways other than SA. For example, BABA is also protective against two necrotrophic pathogens, *Alternaria brassicicola* and *Plectosphaerella cucumerina*, while BTH has no significant effect on resistance against them (Ton and Mauch-Mani, 2004). BABA-IR against *A. brassicicola* and *P. cucumerina* was unaffected in the JA-insensitive mutant *coi1-1* and the camalexin-deficient mutant *pad3-1*. Moreover, the expression of BABA-IR was not associated with enhanced accumulation of camalexin or enhanced transcription of the JA-inducible *PDF1.2* gene. Instead, BABA-IR was blocked in the ABA-deficient mutant *aba1-5*, the ABA-insensitive mutant *abi4-1* and the callose-deficient mutant *pmr4-1*. This suggests that ABA signaling and related callose deposition are involved in the regulation of BABA-induced priming against necrotrophic pathogens.

Last year in our lab, we found that BABA-IR to heat stress and *Pst* DC3000 was abolished by L-glutamine treatment (Wu et al., 2010). As reported, all amino acids, except for L-glutamine, cause one unfamiliar phenomenon called general amino acid inhibition, which is prevented by L-glutamine (Bonner et al., 1996; Bonner and Jensen, 1997).

Together, these studies suggest that BABA pretreatment probably induced a stressed state in plants by yet unknown mechanisms, which might be linked with activation of various downstream defense responses against different biotic or abiotic stresses.

Objectives

During this master, I investigated BABA-IR to the bacterial pathogen *Pst* DC3000 and the mechanism of BABA priming upon bacterial infection. Related researches on this topic had only focused on SA signaling and downstream *PR1* expression (Zimmerli et al., 2000). To understand what might happen upstream or earlier than these events, plant innate immunity under BABA pretreatment was examined, including PTI-responsive genes expression and callose deposition. In addition, to further understand molecular basis of BABA-IR and to use BABA as a tool to identify novel genes involved in the Arabidopsis immunity, mutants screening experiments were conducted. A brief analysis of the candidate mutants is also presented.

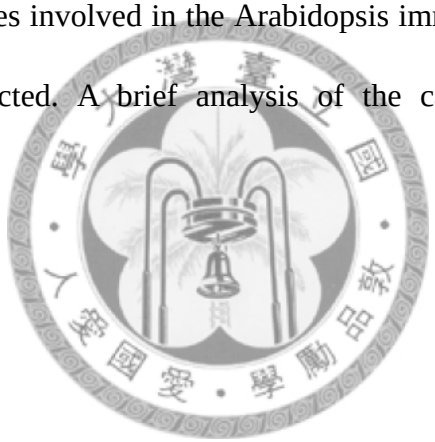

Material and Methods

Plant Material and Growth Conditions

Arabidopsis thaliana plants, wild type Columbia (Col-0), *sid2-1* (AT1G74710), *atnudx25* (At3g10620; SALK_00093), *lrr-pk-1* (AT3G21340; SALK_000388), and *lrr-pk-2* (CS000992) Arabidopsis plants were grown on soil mix of soil/ perlite (3:2) with one plant per pot (6 × 6 × 5cm), in a growth chamber at 22°C day and 18°C night with 9-h photoperiod per 24 h for 5 weeks.

Screening of Homozygous Mutant Plants

T-DNA insertion mutants in this study were derived from the Arabidopsis Biological Resource Center (ABRC). To isolate homozygote of T-DNA insertion mutants, at least 10 seeds of each line were grown in long day condition for later genotype assay and seeds collection.

Genomic DNA was prepared as follow. Rosette leaves from two-week-old plants were collected from each plant and DNA was then extracted as described previously (Edwards et al., 1991). Briefly, leaf samples were extracted with 400 µl of extraction buffer (200mM Tris-HCl pH7.5, 250mM NaCl, 25mM EDTA, 0.5% SDS) and were vortexed shortly. The mixture was then centrifuged at 14,800 rpm for 1 min. 300 µl of supernatants were transferred to new 1.5-mL microcentrifuge tubes and mixed with equal volume of isopropanol. The samples were left at room temperature for 2 min and centrifuged at 14,800rpm for 5 min. The pellets were air dried at 55°C. Fifty µl of filtered water was added to dissolve the pellet. DNA samples were kept in -80°C for long term storage or 4°C for immediate genotype assay.

The genotype assay was done with two sets of PCR analyses. In the first set of PCR, gene-specific primers (LP and RP, designed by Salk Institute Genomic Analysis Laboratory (SIGnAL) website http://signal.salk.edu/) were used to amplify the gene fragment without T-DNA insertion. The second set of PCR using RP primer and T-DNA left border of the vector as a primer, which were to identify the presence of T-DNA insertion. The homozygous lines have insertions in both chromosomes, and won't get any product in first PCR, but one single band in second PCR. The seeds of homozygous plants were then collected for further experiments. The primers used in this study are listed in Table 2.

Plants Treatments

Five-week-old Arabidopsis plants were used for all treatments. For BABA-induced resistance assay, BABA (Sigma-Aldrich) treatments were performed as soil drench applications at 225 μM final concentration. Control plants were treated with an equal volume of water. Pathogen infection experiments were performed 48 h after BABA treatment.

For flg22-induced resistance assay, treatments with flg22 (Biomer Technology) were performed by pressure infiltration (needle-less) of 1 μM peptide solution into leaves. Control plants were infiltrated with 10 mM $MgSO_4$ buffer solution. Pathogen infection experiments were performed 24 h after flg22 treatment.

In the combined assay of BABA and flg22-induced resistance, plants were first treated with BABA for 48 h, and then infiltrated with flg22 for 24 h before pathogen infection experiment.

For gene expression analysis, flg22 at 100 nM were applied for the indicated times.

Pseudomonas syringae Infection and Bacterial Growth Assay

Pseudomonas syringae pv *tomato* strain DC3000 and DC3000 *hrcC*$^-$ mutant were grown during 16-18 h at 28 °C in King's B medium with 100 μg ml^{-1} of rifampicin (*Pst* DC3000) or 100 μg ml^{-1} of rifampicin and kanamycin (*Pst* DC3000 *hrcC*$^-$). Bacteria were then resuspended in 10 mM $MgSO_4$ with OD_{600} value at 0.2 corresponding to concentration of 10^8 cfu ml^{-1}. For dipping inoculation, bacterial densities were adjusted to 5×10^6 c.f.u. ml^{-1} or 2×10^7 c.f.u. ml^{-1} for bacterial growth assays or gene expression analysis, respectively, or as indicated in the figure legends. For infiltration inoculation, bacterial densities were adjusted to 10^5 c.f.u. ml^{-1} for bacterial growth assays, gene expression analysis, and callose depositions, as indicated in the figure legends.

Bacterial growth assays were performed as previously described (Zimmerli et al., 2000) with the following modifications. *Pst* DC3000 bacterial suspensions were either dip- or infiltrated-inoculated into 5-week-old plants after indicated pretreatment of flg22, BABA, or mock control. Each sample consisted of nine leaf discs (5 mm diameter) from three plants (three leaves each). Leaf discs were homogenized in 1.5 ml of 10 mM $MgSO_4$ and dilution series were made. Fifty μl of appropriate dilutions were applied on King's B plates containing 100 μg ml^{-1} of rifampicin. Tissue samples were harvested from inoculated leaves at 2, or 3 dpi for dip-inoculation or at 0, 2, or 3 dpi for infiltration-inoculation experiments, as indicated in the figure legends.

Botrytis cinerea Infection

Botrytis cinerea was grown on 1/2 PDA-agar plates for 14 d. Spores were washed out from plates with proper amounts of 1/2 PDB medium and quantified with a hemocytometer. Spores were then diluted to 10^5 spores ml^{-1} in 1/2 PDB medium. Ten μl of spore suspension were inoculated on leaf surfaces of five-week-old plants (three leaves per plants). Disease symptoms were determined at 3 or 5 dpi, as indicated in the figure legends.

Erwinia carotonova Infection

Erwinia carotovora subsp. *carotovora* strains WPP14 was grown during 16-18 h at 28°C in Luria-Bertani (LB) medium without antibiotics. Bacteria were then resuspended in 10 mM $MgSO_4$ with OD_{600} value at 0.25 corresponding to concentration of 10^8 c.f.u. ml^{-1}. Bacterial densities were adjusted to 3×10^5 c.f.u. ml^{-1} for dipping inoculation of 5-week-old plants. Disease symptoms were determined at 2-4 dpi, as indicated in figure legends.

Callose Deposition

Five-week-old plants were injected with 10^7 c.f.u. ml^{-1} of *Pst* DC3000 suspension or 1 μM of flg22, and samples were collected at indicated time points. Control plants were infiltrated with 10 mM $MgSO_4$ buffer solution. Leaf discs (5 mm diameter) excised from infiltrated leaves were cleared overnight in 96% ethanol until leaf discs appeared white and slightly transparent. Leaf discs were washed twice with

water for 2 h each time. After washing, leaf discs were incubated with 70 mM Na_2HPO_4 (pH 8.0) solution containing 0.05% aniline blue overnight. Callose deposits were visualized using Olympus EX51 microscope under UV illumination with broadband DAPI filter set.

Pictures of random areas of leaf discs were taken and callose deposits were counted using the "analyze particles" of ImageJ (http://rsbweb.nih.gov/ij/). Nine leaf discs from different leaves of three plants were analyzed for each treatment or genotype.

RNA Extraction and Gene Expression Analysis

Total RNA was extracted from leaf tissue or whole plant with the RNeasy Plant Mini Kit (Qiagen). Contaminating DNA was removed with an RNase-free DNase Set (Qiagen), and RNA concentrations were quantified with a Nanodrop Spectrophotometer (Thermo Scientific). RNA samples were diluted to equal concentrations of 2 μM before synthesis of cDNA with M-MLV reverse transcriptase (Invitrogen).

Real-Time and semi-quantitative RT-PCRs were performed using the primers listed in Table 1. *EF1α* (AT5G60390) was used as the internal reference. Real-Time RT-PCR experiments were carried out using an iQ5 Real-Time PCR Detection System (Bio-Rad) and the KAPA SYBR® FAST qPCR Kits (Kapa Biosystems), following the manufacturer's protocol. The thermal cycling program used was an initial 95 °C for 3 min, followed by 40 cycles at 95 °C for 3 s, 60 °C for 30 s. Melting curve was run from 65 °C to 95 °C with 10 s time intervals to ensure the specificity of the product.

Data were analyzed using the Bio-Rad iQ5 software (version 2.0).

Mesophyll Protoplast Transient Expression Assay

Protoplasts were prepared essentially as described previously (Yoo et al., 2007). Leaves from 5-week-old plants were cut into strips and transferred immediately into fresh prepared enzyme solution (20 mM MES (pH 5.7) containing 1.5% cellulose R10 (Yakult Pharmaceutical Ind. Co.), 0.3% mecerozyme R10 (Yakult Pharmaceutical Ind. Co.), 0.4 M mannitol, 20 mM KCl, 10 mM $CaCl_2$ and 0.1% BSA). Leaf strips were incubated for 2-2.5 h. Protoplasts were collected carefully into 5-ml centrifuge tubes and centrifuged at 100 g for 1 min at room temperature. Supernatant was removed and 3-4 ml of W5 solution (2 mM MES (pH 5.7) containing 154 mM NaCl, 125 mM $CaCl_2$ and 5 mM KCl) was added to wash the protoplasts. Centrifugation was repeated once and protoplasts were resuspended in 2-5 ml W5 solution, and then kept on ice for 30 min (or 4 °C overnight). After protoplasts were settled at bottom of tube by gravity, W5 solution was removed and resuspended with equal volume of MMG solution (4 mM MES (pH 5.7) containing 0.4 M mannitol and 15 mM $MgCl_2$). DNA plasmid and 100 µl protoplasts were added into a 2-ml centrifuge tube and mixed with equal volume of PEG by gently tapping the tube. Mixture was incubated at room temperature for 15 min, and then diluted with 440 µl W5 solution, and centrifuged at 100 g for 2 min at room temperature. Supernatant was removed and added with 100 µl of W5 solution. Protoplasts was incubated overnight and kept under light at room temperature. The fluorescence was observed with a TCS SP5 confocal fluorescence microscope (Leica).

DNA Constructs

The vector for the expression of self-complementary RNA (termed hairpin) targeted to *PR2* (AT3G57260) were constructed using Gateway cloning technology (Invitrogen). 393 bp of cDNA fragment encoding partial open reading frame of *PR2* was chosen following the rule that blocks of sequence identity with non-target gene of over 20 bases should be avoided. This short fragment were subcloned into the donor vector, pDONR221, and then recloned into the destination vector, pB7GWIWG2(I), in which inverted repeat of *PR2* gene fragments separated by a spacer sequence was expressed as hairpin structure under the control of the cauliflower mosaic virus 35S promoter. The *PR2* fragment sequence and specific primers for PCR amplification are listed in Table 3. PCR and *in vitro* BP and LR recombination reactions were carried out according to the manufacturer's instructions (Invitrogen).

The DNA plasmids which express LRR-PK protein fused with GFP (S3G21340HGF) or Flag epitope tag (S3G21340BFF) at their C termini under the control of the cauliflower mosaic virus 35S promoter were obtained from the Arabidopsis Biological Resource Center (ABRC) and were as described (Gou et al., 2010).

Agrobacterium tumefaciens (strain GV31), which was transformed with constructs obtained by electroporation, was used for the transformation of Col-0 wild-type plants (with LRC1, S3G21340HGF, S3G21340BFF), *sid2* (with LRC1), and *lrr-pk-2* (with S3G21340HGF, S3G21340BFF) mutant lines. The seeds with successful transformation were screened on 1.5% MS agar plates containing 50 μM

glufosinate-ammonium (Fluka). T2 plants were transferred onto soil for bacterial growth assay and seed collection.

Results

BABA-Induced Resistance to *Pst* DC3000 in the SA Biosynthetic Mutant *sid2*

As suggested by Zimmerli *et al.*, 2000, BABA-induced resistance to *Pst* DC3000 essentially depends on potentiation of the SA-signaling. *SID2* (*SALICYLIC ACID INDUCTION DEFICIENT 2*) encodes an isochorismate synthase required for SA synthesis. It has been reported that *PR1* expression in *sid2* is highly reduced after infection with *Pst* DC3000 avirulent strain (Nawrath and Metraux, 1999). Interestingly, when *sid2* was inoculated with low concentration (5×10^6 c.f.u. ml^{-1}) of *Pst* DC3000 with dipping method, BABA still provided protection in the mutant (Figure 1A). In bacterial growth assay, BABA pretreated *sid2* demonstrated a 2-7 times reduction in bacterial growth (Figure 1B), while in wild-type Col-0, the BABA-pretreated plants demonstrated 8-10 times reduced bacterial growth (Figure 1B). We also examined bacterial growth by syringe infiltration of 10^5 c.f.u. ml^{-1} *Pst* DC3000. In two biologically independent replicates, although BABA-pretreated wild-type Col-0 still exhibited less bacterial growth, BABA-pretreated *sid2* demonstrated a similar bacterial growth compared to water-pretreated controls (Figure 1C). Therefore, the difference of bacterial growth in *sid2* mutant caused by BABA pretreatment was predominately observed when bacteria were inoculated with the dipping method.

BABA Pretreatment Alters Gene Expression during Plant Innate Immunity

To investigate BABA effects on plant innate immunity and its relationship with

SA signaling, we examined the expression levels of several innate immunity marker genes in wild type and *sid2* mutant. The marker genes chosen included genes specific for the MAPK cascade, *FRK1* and *WRKY53* (Asai et al., 2002), genes reflecting activation of CDPK cascade, *CYP81F2* and *NHL10* (Boudsocq et al., 2010), and gene upstream of SA production and signaling, *CBP60g* (Wang et al., 2009). Basal gene expression levels were analyzed 48 h after BABA pretreatment. In wild type and *sid2*, most of the five selected genes were induced by BABA pretreatment (Figure 2A). Expression levels of these genes were examined following *Pst* DC3000 *hrcC* or flg22 treatment. *Pst* DC3000 *hrcC* lacks functional type three secretion system (TTSS) to overcome plant innate immunity, and largely induces PAMP-triggered immunity during infection (Tsuda et al., 2008). In these experiments, buffer infiltrated samples were used as controls. Following either *Pst* DC3000 *hrcC* or flg22 treatment, all the five genes demonstrated higher expression levels in BABA pretreated plants (Figure 2B to G). BABA pretreated *sid2* demonstrated similar expression pattern as Col-0 wild type.

Hence, basal and induced levels of plant innate immunity marker genes were both positively regulated by BABA pretreatment. And this regulation was independent of SA signaling.

BABA Pretreatment Alters Callose Deposition During *Pst* DC3000 Infection

Callose deposition, another classical marker of plant innate immunity, was also analyzed following inoculation with *Pst* DC3000. Callose accumulated in bacteria-inoculated plants but not in buffer-infiltrated mocks (Figure 3A and B). At 6

hpi and 9 hpi with bacteria, water pretreated *sid2* always exhibited less callose deposition than water pretreated wild type (Figure 3A and B). Notably BABA pretreated wild type and *sid2* both showed higher callose deposition than water pretreated controls (Figure 3A and B).

Beside difference in density of callose deposits, morphologically distinct type of callose deposition was also observed in BABA pretreated plants (Figure 3C, D and E). BABA pretreated plants contained normal and big callose deposits. To analyze this phenomenon, diameter of callose was analyzed using 20 μm as criterion to distinguish between small and big callose, as described by (Ham et al., 2007). Deposits of callose greater than 20 μm in diameter are classified as big, those less than 20 μm are classified as small. Big callose accumulated only in BABA pretreated plants, and was most prominent at 9 hpi with bacteria, but the diameter of big callose never exceeded 40 μm (Figure 3C, D and E).

MYB51 encodes a transcription factor downstream of ethylene (ET) signaling and is induced in response to PAMPs treatment (Clay et al., 2009). *MYB51* is usually considered as a marker gene for callose deposition (Clay et al., 2009; Millet et al., 2010). Interestingly, higher expression was observed in BABA pretreated wild type and *sid2* after either flg22 or *Pst* DC3000 *hrcC* inoculation (Figure 3F and G).

Hence, enhanced callose accumulation with BABA pretreatment was related to BABA priming of plant innate immunity marker gene.

BABA Pretreatment Does Not Change Flg22-Induced Resistance

Flg22 pretreatment can induce resistance to subsequent bacterial infection, a

phenomenon very similar to BABA-IR. In previous result, we observed that BABA positively regulates flg22 or *Pst* DC3000 *hrcC* induced gene expression and callose deposition. Hence BABA pretreatment may also demonstrate some effects on flg22-IR. Therefore, plants were pretreated with BABA and then treated with flg22 and subsequently inoculated with *Pst* DC3000. At 4 dpi with bacteria, plants with flg22 or BABA or both pretreatment were less infected than non-pretreated plants (Figure 4A). But disease severity among the three pretreatment conditions was nearly identical. To more precisely examine the symptom, bacterial growth at 2 dpi was assessed. Compared to BABA pretreatment, flg22 pretreatment more efficiently reduced bacterial growth (Figure 4B). And BABA pretreatment did not induce more flg22 protection (Figure 4B). This result suggests that signaling events of BABA-IR and flg22-IR may overlap with each other.

Generation of *PR2* Gene Silencing Transgenic Line in *sid2* Background

As reported, *PR1* expression levels are strongly reduced in *sid2* after pathogen attack, while *PR2* expression levels remain normal (Figure 5) (Nawrath and Metraux, 1999). The BABA-IR observed in *sid2* may thus be due to BABA up-regulation of *PR2*, which in turn slightly increase resistance to pathogen infection. To test this hypothesis, we reduced *PR2* expression in *sid2* by using the gene silencing approach. The Gateway destination vector pB7GWIWG2(I) was used to design gene silencing constructs (Figure 6A). Over-expression of *PR2* inverted repeat separated by intron spacer was cloned into pB7GWIWG2(I), and named as LRC1 (Figure 6A). Restriction enzyme EcoRI and XbaI were used to examine insertion of *PR2* fragments.

In LRC1, both recognition sites of EcoRI were replaced by *PR2* fragments, hence the plasmid was not cleaved by enzyme (Figure 6B). On the other hand, XbaI digested product of LRC1 demonstrated reduced size as predicted (Figure 6B). Furthermore, insertion of *PR2* fragments was examined by two sets of PCR analysis. In first set of PCR, 35S promoter and *PR2* primers were used to amplify first *PR2* fragment (Figure 6C). The second set of PCR used *PR2* and 35S terminator primers to identify the reversely inserted *PR2* fragment (Figure 6C). Twenty-six putative T1 lines were selected for segregation analysis. Among them, 21 T2 lines had survival rates more than 70 % on MS medium containing BASTA, which were either heterozygous or homozygous for *PR2* silencing construct. These lines were then assayed for their *PR2* expression in response to *Pst* DC3000 infection. At least 5 lines (line number 1, 7, 8, 10, 25) demonstrated reduced *PR2* expression (Figure 7A). The transgenic lines possess more widely expanded leaves and shorter petioles (Figure 7B).

Bacterial growth was assayed to determine whether *PR2* plays an important role in the BABA-IR observed in the *sid2* mutant. Preliminary tests indicated that most of the BABA-pretreated transgenic lines demonstrated a response similar to *sid2* (Figure 8A and 8B). This preliminary observation suggests that BABA-IR in *sid2* can function independently of *PR2*.

Knock-out Mutant Lines Screening

To evaluate the effects of BABA on Arabidopsis, gene expression was monitored 24 h after BABA treatment with the microarray approach (Zimmerli et al., 2008). Among the genes with altered expression levels, 678 genes were found to be

up-regulated in response to BABA, whereas only 83 genes were repressed (Zimmerli *et al*., 2008). To understand whether these candidate genes might be involved in BABA-IR against *P. syringae* or other pathogens, and also to investigate their roles in the plant innate immunity, a group of genes encoding receptor like kinases and enzymes were selected from the microarray data, and their T-DNA mutant lines were ordered from ABRC for further studies. Bacterial infection symptoms were observed 3 days after infection. The disease rates of wild-type and mutant plants were compared. Mutant sensitivities towards BABA pretreatment were also examined. With massive screening of near 70 mutant lines, two T-DNA mutants demonstrated interesting phenotype. The first is a knock-out mutant line of *AtNUDX25* gene; the second interesting line is a knocked out of a putative leucine-rich repeat protein kinase (LRR-PK). Both mutant lines were described in detail in the following sections.

Sequence Analysis of *AtNUDX25* and Identification of *atnudx25* mutant

AtNUDX25 consists of five exons. The full length CDS contains 528 bp which encodes a 175-residue peptide. The conserved Nudix motif (residues 40 to 62) is shown in Figure 9A and together compared with the sequence of the well-characterized plant Ap_4Aase from *Lupinus angustifolius*. A Tyr residue 15 amino acids downstream of the Nudix box is considered responsible for the preference of Ap_4A as enzyme substrate (Dunn et al., 1999) (Figure 9A).

T-DNA mutant lines of *AtNUDX25* were ordered from ABRC. T-DNA insertion sites are as indicated (Figure 9B). SALK_00093, has a T-DNA insertion in its third

intron at 240 bp 3' to the initial codon. Another T-DNA mutant (SALK_078741) has T-DNA insertion in 5' UTR. Knock-out of *AtNUDX25* was examined by RT-PCR. *AtNUDX25* transcript was knocked out in SALK_00093 (hereafter referred to as *atnudx25*), but not in SALK_078741 (Figure 9C). Therefore, for the following experiments, *atnudx25* was used as the only loss-of-function mutant of *AtNUDX25*.

Mutation in *AtNUDX25* Result in Enhanced Susceptibility to Necrotrophic Pathogens

atnudx25 were more severely infected by two necrotrophic pathogens, the fungal pathogen *B. cinerea*, and the bacterial pathogen, *Ecc* WPP14 (Figure 10A and 11). The lesion size of *B. cinerea* infected leaves was determined 3 days after inoculation. The diameter was larger in *atnudx25* mutant than wild type (Figure 10B).

Both of the pathogens kill host cells at very early stages in the infection and cause extensive tissue damage. They induce jasmonates (JA)-dependent defense responses in plant (Glazebrook, 2005), therefore we analyzed the marker gene for JA signaling, *PDF1.2*, following pathogen inoculation. The preliminary studies indicated that the basal expression of *PDF1.2* (0 hpi) was higher in *atnudx25* (Figure 10C). But after inoculations of *B. cinerea*, *PDF1.2* expression was normally induced (Figure 10C). Therefore, although enhanced susceptibility was observed, reduction in JA downstream marker gene, *PDF1.2*, expression was not detected in our test. This preliminary result suggests that *AtNUDX25* functions independently of JA signaling.

Mutation in *AtNUDX25* Does Not Affect Response to flg22 and *Pst* DC3000

According to the web database, BAR (The Bio-Array Resource for Plant Functional Genomics) (http://bar.utoronto.ca/), *AtNUDX25* is induced in response to bacterial PAMP, flg22. At 1hpi with flg22, *AtNUDX25* was highly induced in wild type, but not in its loss-of-function mutant (Figure 12B). To test whether *AtNUDX25* is important for perception of flg22, expression of the PTI marker gene *FRK1*, following flg22 treatment was analyzed. But no significant differences in the gene expression were observed between wild type and mutant (Figure 12C).

Sensitivity of *atnudx25* mutant to hemi-biotrophic bacteria such as *Pst* DC3000 was also assessed. *Pst* DC3000 contains flg22 PAMPs in their flagella. The disease rates of wild type and *atnudx25* were quite similar (Figure 12A). These results suggested, while *AtNUDX25* responses quickly upon perception of flg22, it might not be involved in plant resistance to *Pst* DC3000.

The Putative *LRR-PK* organization and Identification of *lrr-pk* mutants

The putative *LRR-PK* consists of twelve exons. The full length CDS contains 2685 bp which encodes an 894-residue peptide. As predicted by the Pfam protein families database (http://pfam.sanger.ac.uk/) (Finn et al., 2010), the N terminus contains a secretion signal peptide (residues 1 to 23) followed by an extracellular domain of unknown function and 2 LRR motifs (residues 409 to 455). A transmembrane domain (residues 512 to 536) is predicted to separate the extracellular domain from intracellular Ser/ Thr kinase domain (residues 587 to 854) (Figure 13A).

T-DNA insertion mutant lines were ordered from ABRC. The insertion sites are

as indicated (Figure 13B). Both *lrr-pk-1* (Salk_000388) and *lrr-pk-2* (CS000992) have T-DNA insertions in regions encoding the kinase domain. RT-PCR was performed to confirm that the T-DNA and transposon insertion inhibited the accumulation of putative *LRR-PK* transcript. Both *lrr-pk-1* and *lrr-pk-2* mutant lines were knocked out of *LRR-PK* (Figure 13C), and were used in the following experiments.

Mutation in the Putative *LRR-PK* Causes Partial BABA Insensitivity and Enhanced Susceptibility to *Pst* DC3000.

We investigated the possible role of the LRR-PK under study by testing the phenotype of *lrr-pk-1* and *lrr-pk-2*. At 3 day post dip-inoculation with *Pst* DC3000 both of the mutant lines showed more yellowing and necrosis than wild-type Col-0 (Figure 14A). In addition, BABA pre-treatment on mutant lines did not provide significant protection against bacterial infection (Figure 14A). In addition, both *lrr-pk-1* and *lrr-pk-2* demonstrated higher bacterial growth than wild type at 2 dpi, (Figure 14B). Interestingly, BABA pretreatment on both mutant lines induced less protection than on Col-0 wild type (Figure 14B). This result suggested that the two mutant lines still respond to BABA pretreatment, but the sensitivity to BABA is reduced.

To understand whether *lrr-pk* mutant lines were defected in early stage of plant innate immunity, bacterial growth following infiltration inoculation of *Pst* DC3000 was assessed. The preliminary result indicated that, when *Pst* DC3000 was directly infiltrated into leaves, *lrr-pk-1* mutant and wild type had similar sensitivity to bacteria (Figure 14C). This suggests that the putative LRR-PK may function during early

stages of Arabidopsis innate immunity.

The Putative *LRR-PK* is Induced in Response to Bacterial Infection and PAMP Perception.

To investigate the role of the putative *LRR-PK* in plant innate immunity, its gene expression in response to bacterial infection and flg22 perception was analyzed. At 3 hpi with bacteria, the putative *LRR-PK* was highly induced by normal *Pst* DC3000 and also TTSS mutated *Pst* DC3000 *hrcC*¯ (Figure 15). Besides, *LRR-PK* was quickly induced by flg22 treatment at 1 hpi (Figure 15). These results suggest that the putative *LRR-PK* has immediate response to bacterial invasion and PAMPs perception as well.

The Putative LRR-PK Localizes to the Plasma Membrane

Protein subcellular localization also may provide information to gene functions. As mentioned, the predicted protein structure of this putative LRR-PK contains one secretion signal peptide targeted to the membrane system and also one transmembrane domain (Figure 13A), therefore we wondered whether this protein really localizes on the plasma membrane in plant cells, which is one feature for many important LRR-PKs involved in plant innate immunity signaling (e.g. FLS2, EFR, BAK1) (Boller and Felix, 2009). The DNA construct, S3G21340HGF, containing the putative LRR-PK CDS fused with a C-terminal GFP, controlled by 35S promoter, was used to transformed Arabidopsis wild-type protoplast.

Under confocal microscope, a clear GFP signal lying on borderline of protoplast was observed, like an annular eclipse (Figure 16). This result suggests that the

putative LRR-PK localizes on the plasma membrane *in vivo*, and further suggests that this protein may function in early signaling of plant innate immunity.

Mutation in the Putative *LRR-PK* Reduces Callose Deposition During *Pst* DC3000 Infection and Flg22 Perception

Callose deposition, another classical marker of plant innate immunity, was also analyzed following inoculation of *Pst* DC3000 or flg22. Buffer infiltrated samples were used as mock controls. At 9 hpi with *Pst* DC3000, callose deposition was strongly reduced in both *lrr-pk-1* and *lrr-pk-2* mutants (Figure 17A and B). Besides, at 12 hpi with flg22, both mutant lines demonstrated reduced callose accumulation (Figure 17A and C). These results suggest that the putative LRR-PK may function in PTI signaling pathway relating to callose deposition.

Discussion

BABA Primes Early Stage of Plant Innate Immunity through Potentiation of Multiple Signaling Pathways

We observed a slightly reduced bacterial growth in BABA pretreated *sid2* mutant when plants were infected by dipping but not by infiltration method (Figure 1). Infiltration of bacteria with syringe might bypass the first steps of the natural infection process, like entering the leaves through natural opening such as stomata (Zipfel et al., 2004). Therefore, we hypothesized that BABA-induced resistance may not only primes the SA signaling but also early steps of plant innate immunity, the so called PTI. It seems that PTI becomes prominent when effects of BABA on SA-signaling were removed, as in the case of *sid2* mutant.

How the early steps of plant innate immunity or PTI interact with downstream SA signaling is one noticeable issue regarding plant defense responses. It is suggested that during PAMPs perception, SA-independent signaling is firstly activated at early stage, which leads to SA accumulation. In turn, plant exploits SA-mediated signaling to maintain PTI (Tsuda et al., 2008). Investigating how BABA primes PTI and probably in turn activating SA signaling may provide new knowledge to this issue.

(A) BABA Primes PTI-Responsive Genes expression

In this study, expression of PTI marker genes was first analyzed, and with BABA pretreatment, 6 PTI-responsive genes demonstrated higher expression levels independently of SA signaling (Figure 2 and 3). SA dependency of these genes is

compared with one previous study which identified several clusters of PAMPs induced genes (PIGs) with characteristic regulatory patterns (Tsuda et al., 2008). Some BABA-primed genes such as *FRK1*, *WRKY53*, *CYP81F2* and *CBP60g* were also reported in this study (Tsuda et al., 2008).

FRK1, *WRKY53* and *CBP60g* are activated independently of SA signaling at early stage of infection, but need SA accumulation to maintain their late expression (Tsuda et al., 2008). Hence, it is reasonable that BABA primes these genes independently of SA signaling at 1 or 3 hpi with flg22 or bacteria. And according to Tsuda *et al*., expression of *CYP81F2* during infection is totally independent of SA, as observed in our study. Besides, PAMPs induce ethylene (ET) production (Felix et al., 1999), Tsuda *et al*. also suggested that a cluster of PAMPs induced genes are regulated by JA/ ET signaling. Previously, BABA was shown to enhance mRNA accumulation of ET early signaling intermediates (Zimmerli et al., 2008). In our study, BABA also primed expression of *MYB51*, the transcription factor downstream of ET signaling (Figure 3F and G). Therefore, BABA pretreatment alters expression of various PTI genes in different signaling pathways. Especially, *CBP60g* primed by BABA is an important component upstream of SA accumulation (Wang et al., 2009), and BABA may prime SA signaling via priming of this PTI gene. In addition, BABA may also manipulate early stage of plant innate immunity through ET signaling, as *MYB51* was also primed by BABA.

(B) BABA Primes Callose Deposition in a SA-independent manner

Other than gene expression, BABA pretreated plants demonstrated enhanced

callose deposition in the *sid2* mutant, thus independently of SA signaling (Figure 3). The early signaling network for callose deposition functions independently of SA. PAMPs or flg22-induced callose can potentiate SA-responsive callose deposition (Clay et al., 2009; Adams-Phillips et al., 2010). Notably, *MYB51* and *CYP81F2*, the genes representing two independent pathways required for flg22-induced callose deposition (Clay et al., 2009), were both primed by BABA. These results thus suggest that BABA enhanced callose deposition is related with MYB51/ET-dependent and CYP81F2/I3G-dependent portions of callose deposition network. Hence, BABA may prime PAMPs or flg22-induced callose deposition and in turn potentiate SA-dependent callose deposition.

On the other hand, BABA pretreated plants frequently demonstrated bigger callose deposits with diameter larger than 20 μm (Figure 3). This morphologically distinct type of callose was also recorded in plant infected with non-host bacterial pathogen, *Pseudomonas syringae* pv. *phaseolicola* (*Pph*) (Ham et al., 2007). Diameter of *Pph* induced big callose ranged from 20 μm to 50 μm. The biological foundation of this phenomenon is not clear, but seems to be independent of SA signaling, as big callose deposition was observed even in SA mutant, *sid2* and *npr1* (Ham et al., 2007). These results suggest that BABA-IR may participate in plant non-host resistance, although the biological mechanism remains elusive.

In summary, BABA primes many flg22 or PAMPs induced defense responses, including gene expression and callose deposition, which are SA-independent in early stage of bacterial infection. Hence, we propose that BABA up-regulates plant defense responses through priming of PTI, and in turn induces SA signaling to continuously

activate plant defense system.

(C) BABA and flg22 Induced Resistance to Bacteria

Although we hypothesized that BABA primes flg22 induced defense responses, however in our preliminary results, BABA pretreatment did not induce more flg22 protection (Figure 4). There are two possible explanations. First, flg22 pretreatment more efficiently reduced bacterial growth than BABA (Figure 4B), and thus BABA-IR is overwhelmed by flg22-IR. Secondly, BABA- and flg22- responsive signaling may be highly overlapped. For example, flg22 induces the production of ET (Felix et al., 1999), and flg22-IR does not strictly depend on SA (Zipfel et al., 2004). Therefore BABA does not provide more protection in flg22-pretreated plants.

AtNUDX25 Regulates Plant Resistance to Necrotrophic Pathogen

Plant responses to necrotrophic pathogens appear to be mediated by a complex web of signaling dominated by JA and ET- signaling pathway (Glazebrook, 2005). In our study, although *atnudx25* mutant demonstrated enhanced susceptibility to necrotrophic pathogens, *B. cinerea* and *Ecc* WPP14, expression of *PDF1.2* expression was similar between *atnudx25* and wild type (Figure 10). This suggests that defect in other signaling pathway leads to more diseased phenotype in *atnudx25*. On the other hand, flg22 highly induced expression of *AtNUDX25* (Figure 12). However, whether *atnudx25* mutant is impaired in flg22 induced responses is yet undetermined. In the future, the relationship between flg22 induced responses and enhanced susceptibility to necrotrophic pathogen in *atnudx25* should be analyzed.

BABA-Induced Plant Resistance against Necrotrophic Pathogen

BABA has been reported to protect plants against a wide range of pathogens, including necrotrophic *B. cinerea* and *Alternaria brassicicola* (Zimmerli et al., 2001; Ton and Mauch-Mani, 2004; Flors et al., 2008). From the microarray data (Zimmerli et al., 2008), BABA effectively induced *AtNUDX25* expression. And in our study, *AtNUDX25* loss-of-function mutant showed enhanced susceptibility to necrotrophic *B. cinerea* and *Ecc* WPP14. This suggests that induction of *AtNUDX25* in BABA-pretreated plants may be related to BABA-induced resistance against necrotrophic pathogen. To verify this hypothesis, further analysis on *atnudx25* mutant responses to *A. brassicicola* and BABA pretreatment are needed.

The Putative LRR-PK Regulates Plant Resistance to Bacterial Pathogen *Pst* DC3000

The *lrr-pk* mutants were more susceptible to *Pst* DC3000 when inoculated by dipping, but not by infiltration (Figure 14). We presume that this putative *LRR-PK* is important for early steps of plant innate immunity. It is first supported by the result that the *LRR-PK* was immediately induced upon bacterial infection and PAMPs perception (Figure 15). Furthermore, transient gene expression assay revealed that LRR-PK protein localizes to plasma membrane *in vivo* (Figure 16). This also supports that the putative LRR-PK functions in early signaling of plant innate immunity. Besides, reduced callose deposition in *lrr-pk* mutants also strongly suggests involvement of this gene in PTI (Figure 17).

On the other hand, this putative LRR-PK was first reported for its responsiveness to flg22 (Zipfel et al., 2004). This gene was induced together with other 27 LRR-PKs (including BAK1) and many other types of receptor-like kinase. Hence, it was speculated that this gene and other receptor-like kinases might be involved in the recognition of other, as yet unidentified PAMPs (Zipfel et al., 2004).

However, our LRR-PK contains only 2 LRR motifs, while the well known LRR-PK, FLS2, contains 28 conserved LRR motifs for flg22 binding. This suggests that our LRR-PK may resemble BAK1 functionally, which contains only 4 LRR motifs and regulates PTI through interaction with other PRR, not by directly binding with PAMPs.

In addition, kinase domains of FLS2 and EFR both belong to non-RD kinases, which contain the sequence CD instead of the normal RD in the catalytic loop of kinase domain, whereas kinase domain of BAK1 and our putative LRR-PK belongs to RD kinases (Dardick and Ronald, 2006). Hence, the kinase domain activity of our protein may be regulated by mechanism similar as BAK1.

The Putative LRR-PK is Involved in BABA Induced Resistance to Bacterial Pathogen *Pst* DC3000

The *lrr-pk* mutants demonstrated reduced BABA-IR to *Pst* DC3000 (Figure 14). We propose that BABA up-regulates plant defense responses through priming of PTI, hence the putative *LRR-PK* may be one essential target of BABA priming. In addition, callose deposition plays an important role in BABA-IR (Figure 3), which is reduced in *lrr-pk* mutants. To verify whether reduced BABA sensitivity in mutants is related

with their deficiency in callose deposition, further analysis is needed. The study on the putative *LRR-PK* provides not only information on the mechanism of BABA priming, but also knowledge of plant innate immunity.

Conclusion and Future Perspectives

BABA is a powerful chemical inducing resistance to *Pst* DC3000. Its pretreatment on plant can trigger induction of many PTI genes upon *Pst* DC3000 infection or PAMP perception. These genes are distributed in various branches of the PTI signaling, including MAPK cascade, CDPK cascade, ET signaling, and SA signaling. It thus suggests that BABA affects early events of plant immune responses by an unknown mechanism common to all these defense signalings. Thus, the previous observation by Zimmerli *et al.* that BABA potentiates *PR1* expression can be explained by our new findings that signaling components upstream of SA signaling accumulated faster with BABA pretreatment, hence *PR1* is induced more quickly and efficiently in response to *Pst* DC3000.

In accordance with gene expression, callose deposition was also primed by BABA pretreatment. This may be related to activation of MYB51/ET-dependent and CYP81F2/I3G-dependent portions of callose deposition network.

On the other hand, in the SA biosynthetic mutant *sid2*, we still observed some BABA-IR to *Pst* DC3000, which can be explained by the SA-independent priming of the PTI response by BABA.

To further understand the mechanism of BABA-IR, we identified two additional genes involved in BABA regulation of plant defense response. AtNUDX25, an Ap_4A hydrolase from Nudix protein family, was induced by BABA pretreatment and was shown important for plant resistance to necrotrophic pathogens, including the fungal pathogen *B. cinerea* and the bacterial pathogen *Ecc* WPP14. So far, little is known

about the physiological function of Nudix protein family in plants and animals. Hence, it is important yet challenging to understand how this protein maybe involved in the plant defense response. In addition, one putative LRR-PK was shown to be important for Arabidopsis resistance to *Pst* DC3000. This protein was also essential for BABA-IR to *Pst* DC3000, as BABA sensitivity was reduced in both of its mutant lines. Confirming our observations that BABA acts at the PTI level, the LRR-PK seems to be involved in early Arabidopsis defense responses. Typically, the LRR-PK is induced by *Pst* DC3000 and PAMPs inoculation, is localized at the plasma membrane, and is defective in callose deposition. In the future, it is important to identify the interplay between this protein and current known PAMPs triggered defense responses or callose deposition.

Besides, LRR-PKs has been shown playing important roles in plant immunity, it is interesting to know whether the putative LRR-PK from our study interacts with some well studied PRRs, BAK1, or other unknown proteins. This may help us to uncover the possible involvement of this LRR-PK in a protein complex involved in the plant innate immunity.

Figures

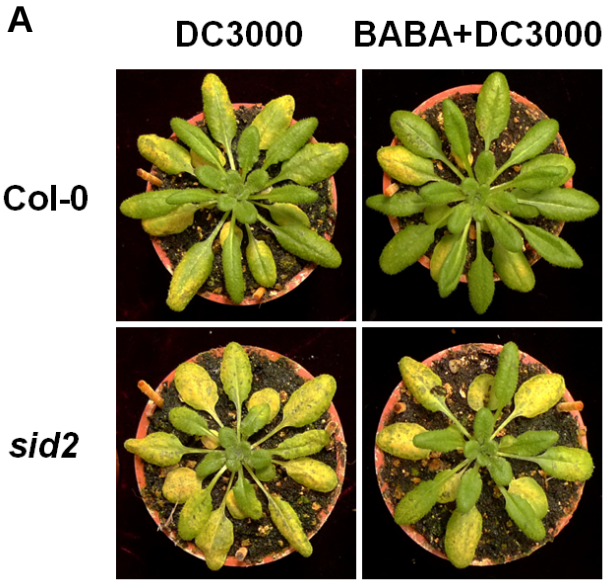
A
DC3000
BABA+DC3000
Col-0
sid2

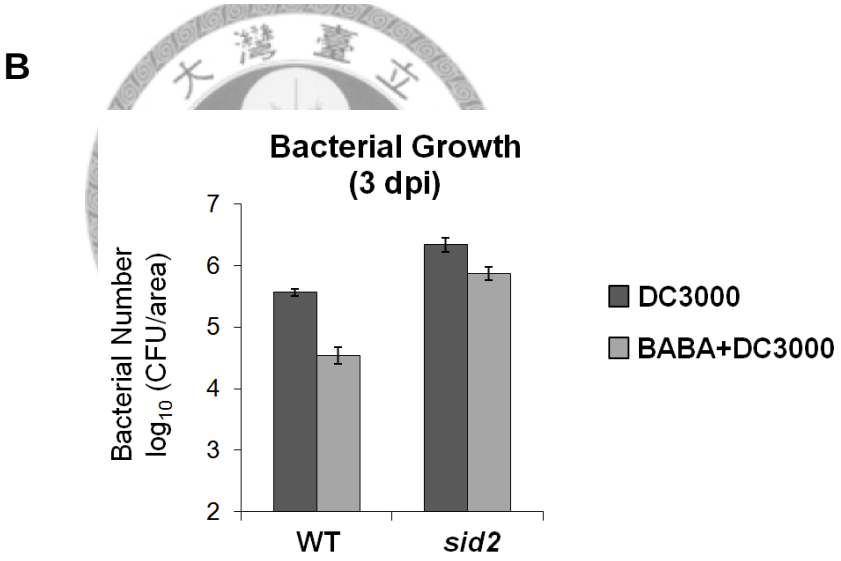
B
Bacterial Growth
(3 dpi)
Bacterial Number
log10 (CFU/area)
7
6
5
4
3
2
WT
sid2
DC3000
BABA+DC3000

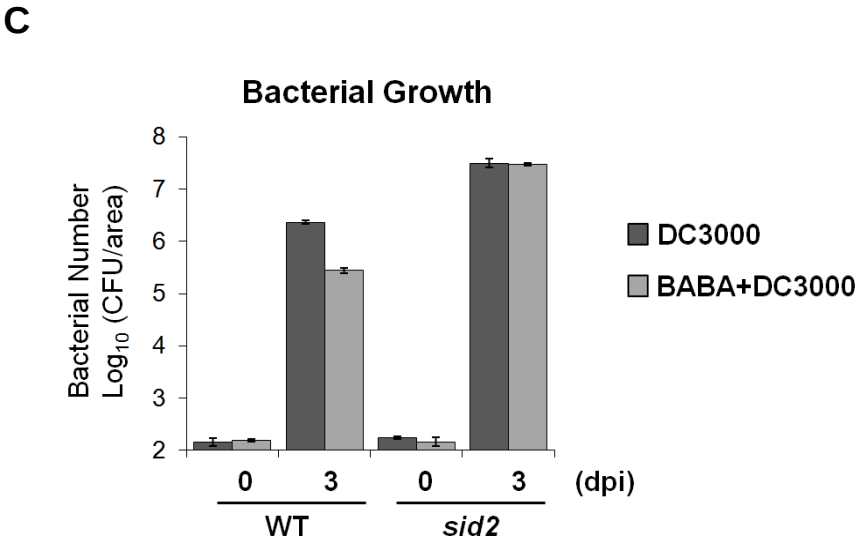
C
Bacterial Growth
Bacterial Number
Log10 (CFU/area)
8
7
6
5
4
3
2
0
3
0
3
(dpi)
WT
sid2
DC3000
BABA+DC3000

Figure1. BABA induced resistance in the SA biosynthetic mutant *sid2*. **A**, Disease symptoms 3 days after *Pst* DC3000 infection. Five-week-old wild-type Col-0 and *sid2* plants were pretreated for 48 h with 225 μM BABA or water control. Subsequently, plants were dip-inoculated with 5×10^6 c.f.u. ml^{-1} bacterial suspension. **B**, Bacterial growth assays 3 days after dip-inoculation of *Pst* DC3000. **C**, Bacterial growth assays 3 days after infiltration-inoculation with 10^5 c.f.u. ml^{-1} *Pst* DC3000. Representative results were shown, with SD of three technical replicates.

A

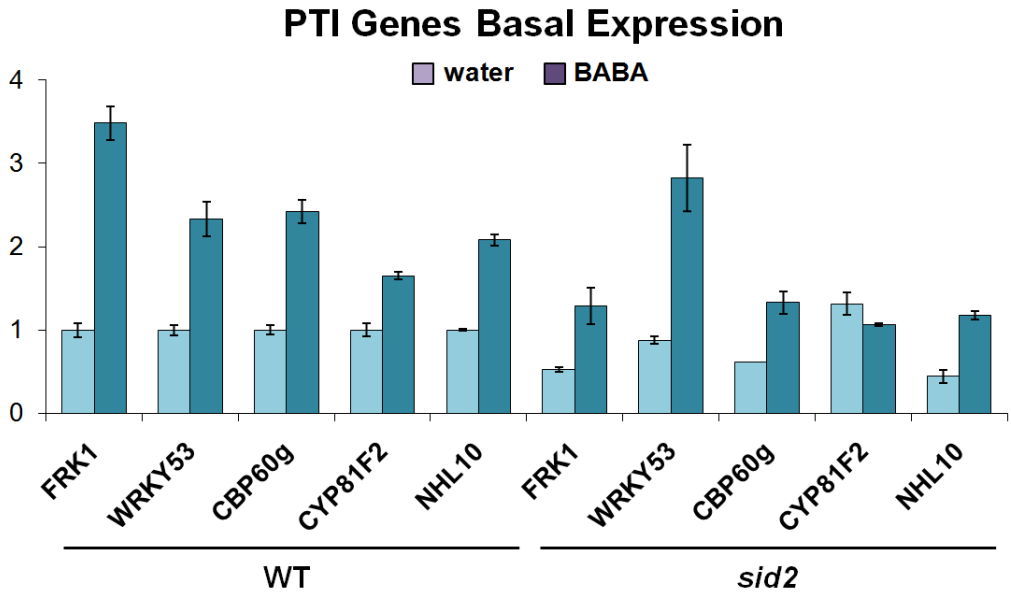
PTI Genes Basal Expression
water
BABA
4
3
2
1
0
FRK1
WRKY53
CBP60g
CYP81F2
NHL10
FRK1
WRKY53
CBP60g
CYP81F2
NHL10
WT
sid2

B

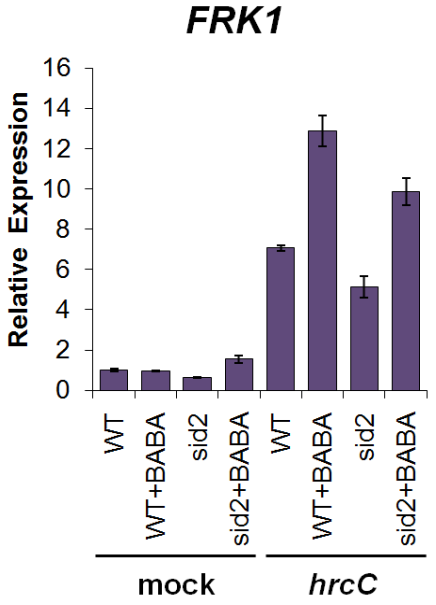
FRK1
Relative Expression
16
14
12
10
8
6
4
2
0
WT
WT+BABA
sid2
sid2+BABA
WT
WT+BABA
sid2
sid2+BABA
mock
hrcC

C

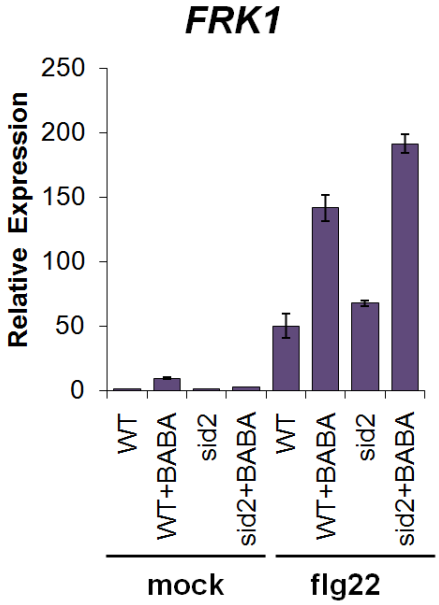
FRK1
Relative Expression
250
200
150
100
50
0
WT
WT+BABA
sid2
sid2+BABA
WT
WT+BABA
sid2
sid2+BABA
mock
flg22

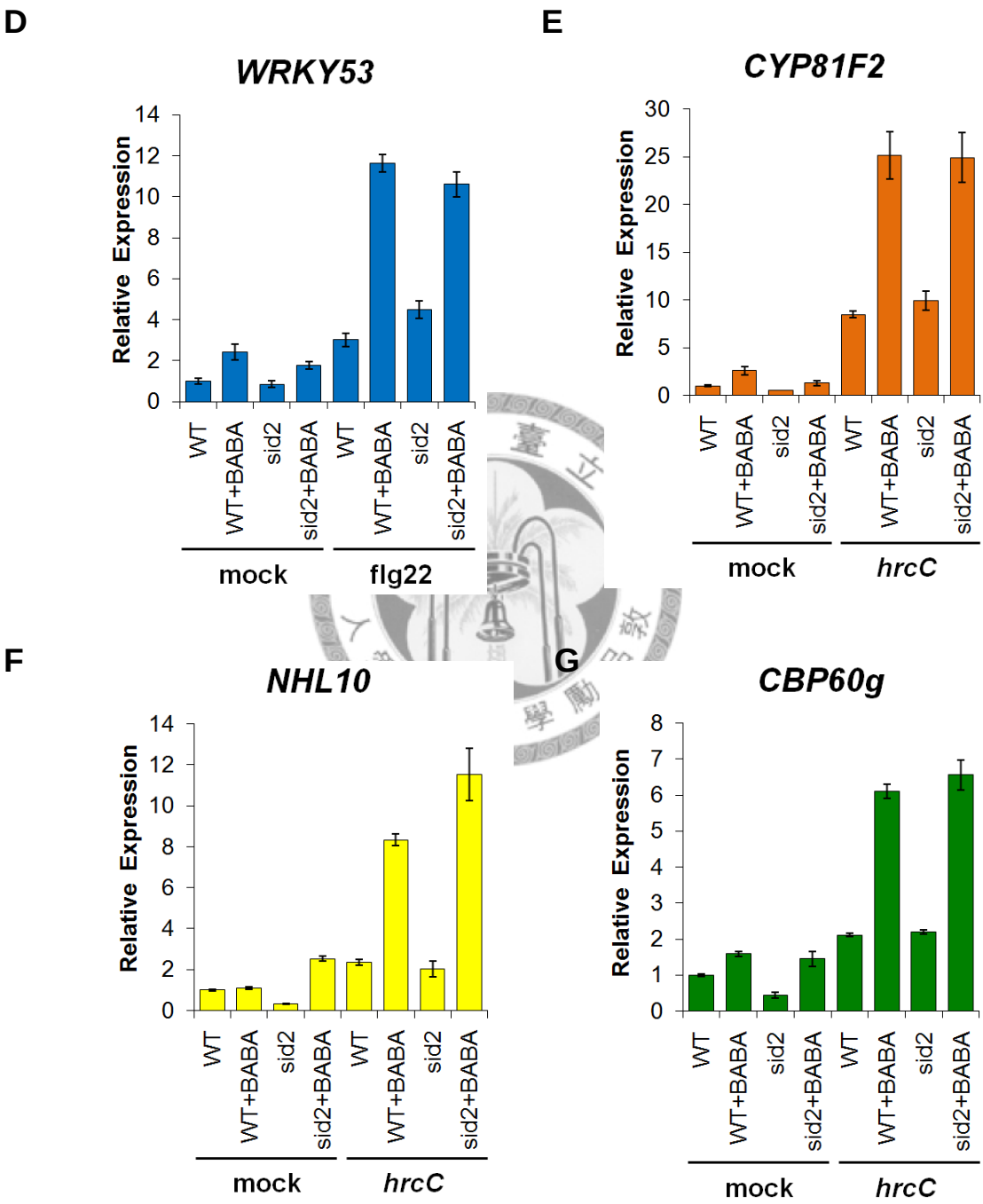
D
WRKY53
Relative Expression
14
12
10
8
6
4
2
0
WT
WT+BABA
sid2
sid2+BABA
WT
WT+BABA
sid2
sid2+BABA
mock
flg22
E
CYP81F2
Relative Expression
30
25
20
15
10
5
0
WT
WT+BABA
sid2
sid2+BABA
WT
WT+BABA
sid2
sid2+BABA
mock
hrcC
F
NHL10
Relative Expression
14
12
10
8
6
4
2
0
WT
WT+BABA
sid2
sid2+BABA
WT
WT+BABA
sid2
sid2+BABA
mock
hrcC
G
CBP60g
Relative Expression
8
7
6
5
4
3
2
1
0
WT
WT+BABA
sid2
sid2+BABA
WT
WT+BABA
sid2
sid2+BABA
mock
hrcC

Figure 2. BABA pretreatment up-regulates plant innate immunity marker genes in basal and induced expressions independently of SA biosynthesis. **A**, Plant innate immunity marker genes basal expression levels following 48 h BABA or water control pretreatment. **B** to **G**, Plant innate immunity marker genes expression in response to 10^7 c.f.u. ml^{-1} *Pst* DC3000 *hrcC* or 100 nM flg22 inoculation (for 3 or 1 h, respectably), following 48 h BABA or water control pretreatment. Mock controls were infiltrated with $MgSO_4$ buffer. The relative expression (fold) is shown, with the *gene*/*EF1* expression values in WT water control (**A**) or WT mock as 1 (**B** to **G**). Representative results were shown, with SD of three technical replicates. Experiments were repeated three times.

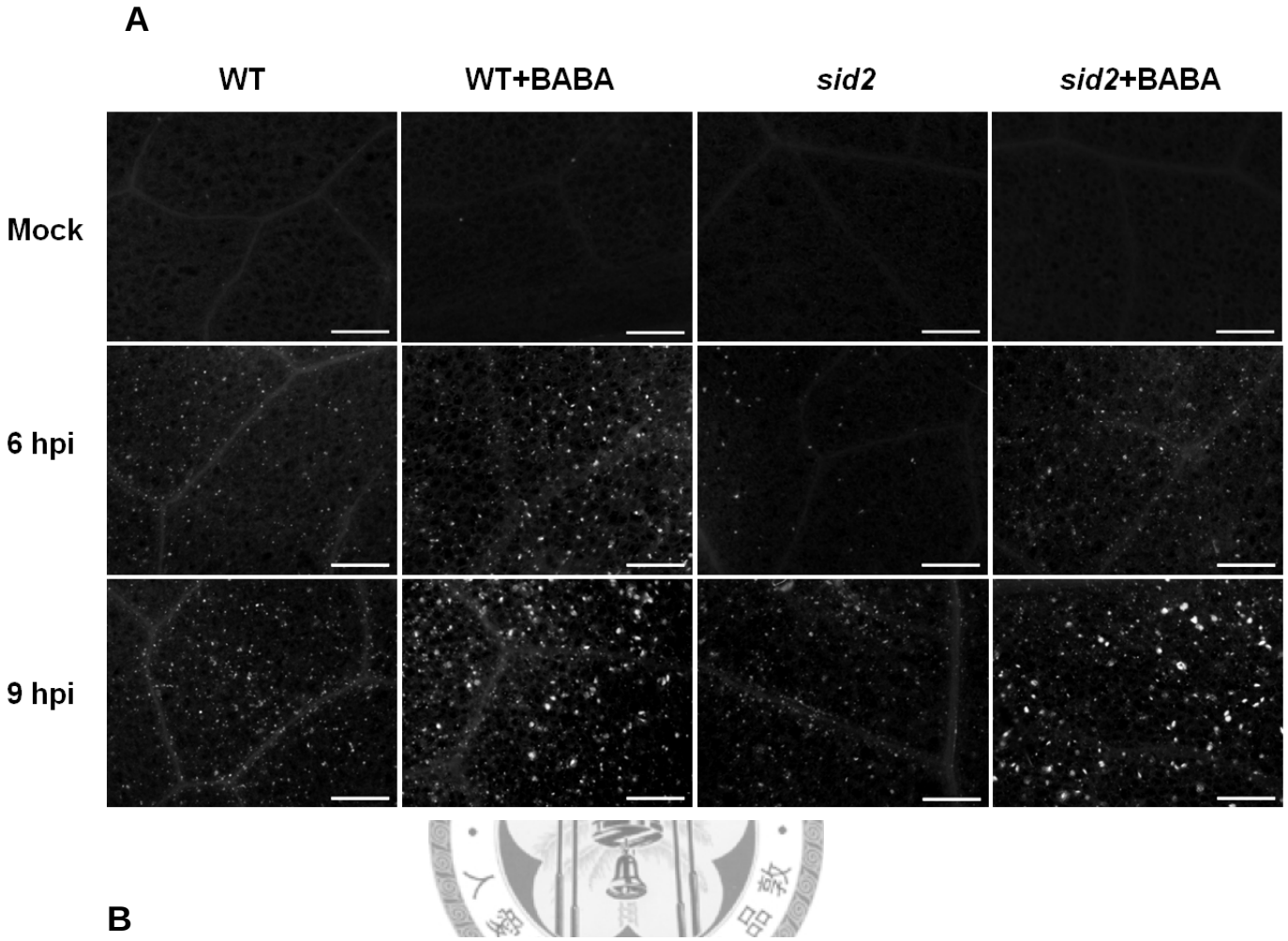
A
WT
WT+BABA
sid2
sid2+BABA
Mock
6 hpi
9 hpi
B
Callose Deposition
Callose Density
(callose deposits/ mm2)
800
700
600
500
400
300
200
100
0
WT
WT+BABA
sid2
sid2+BABA
mock
6 hpi
9 hpi

C

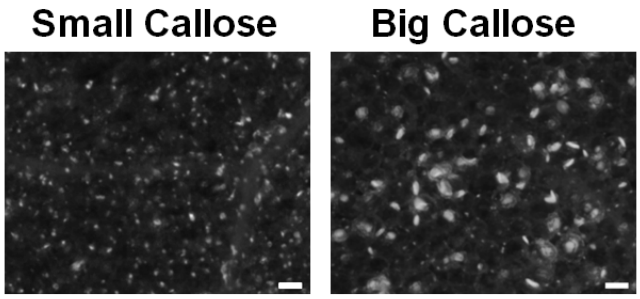
Small Callose
Big Callose

D

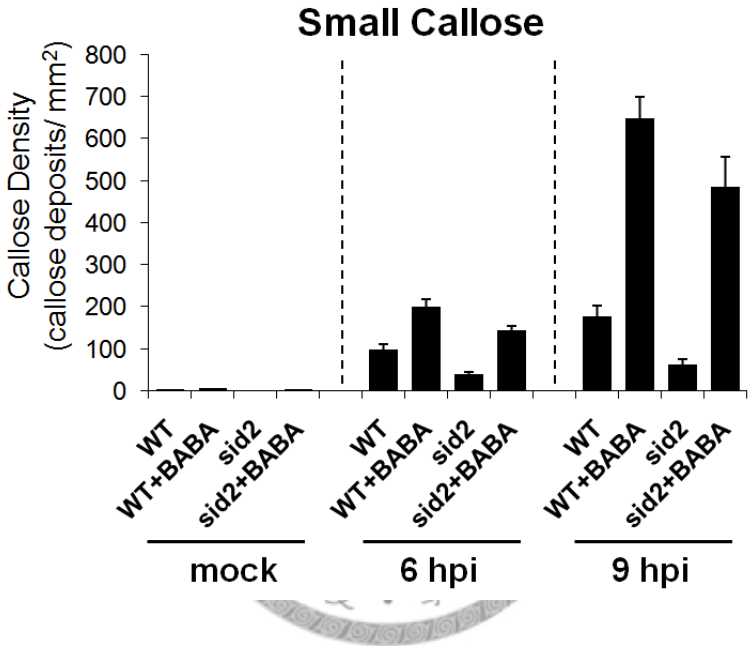
Small Callose
Callose Density
(callose deposits/ mm2)
800
700
600
500
400
300
200
100
0
WT
WT+BABA
sid2
sid2+BABA
mock
6 hpi
9 hpi

E

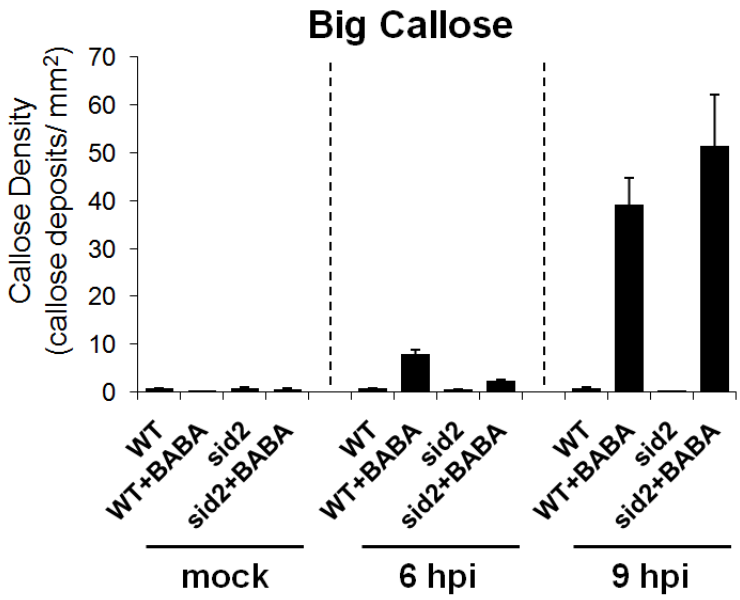
Big Callose
Callose Density
(callose deposits/ mm2)
70
60
50
40
30
20
10
0
WT
WT+BABA
sid2
sid2+BABA
mock
6 hpi
9 hpi

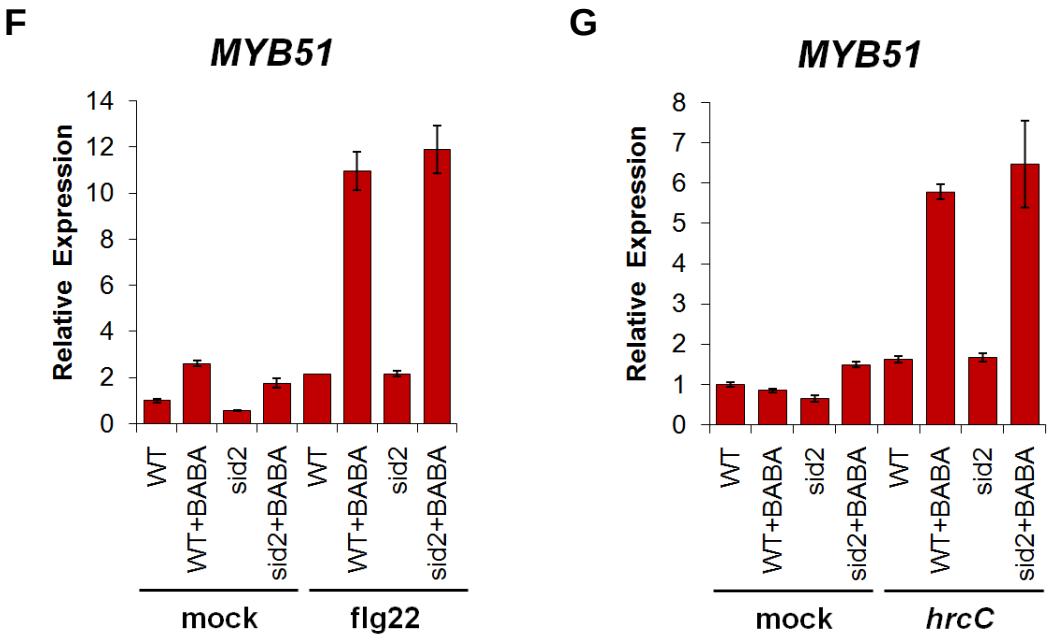

Figure 3. BABA pretreatment enhances callose deposition after *Pst* DC3000 infection independently of SA biosynthesis. **A**, Col-0 and *sid2* plants were pretreated for 48 h with 225 µM BABA. Subsequently, plants were infiltrated with 10^7 c.f.u. ml^{-1} *Pst* DC3000. Samples were collected at indicated time points. White bars equals to 200 µm. **B**, Measurement of callose deposition in response to *Pst* DC3000 inoculation. **C**, Comparison between small and big callose. Deposits of callose greater than 20 µm in diameter are classified as big, those less than 20 µm are classified as small. White bars equals to 40 µm. **D** and **E**, Small and Big callose induced in response to *Pst* DC3000 inoculation. Representative results were shown, with SE of at least 24 measurements. This experiment was repeated three times, and similar results were obtained. **F** and **G**, *MYB51* expression in response to BABA pretreatment and flg22 or *Pst* DC3000 *hrcC* inoculation. Treatment and Real-Time PCR condition were as indicated in Figure 2.

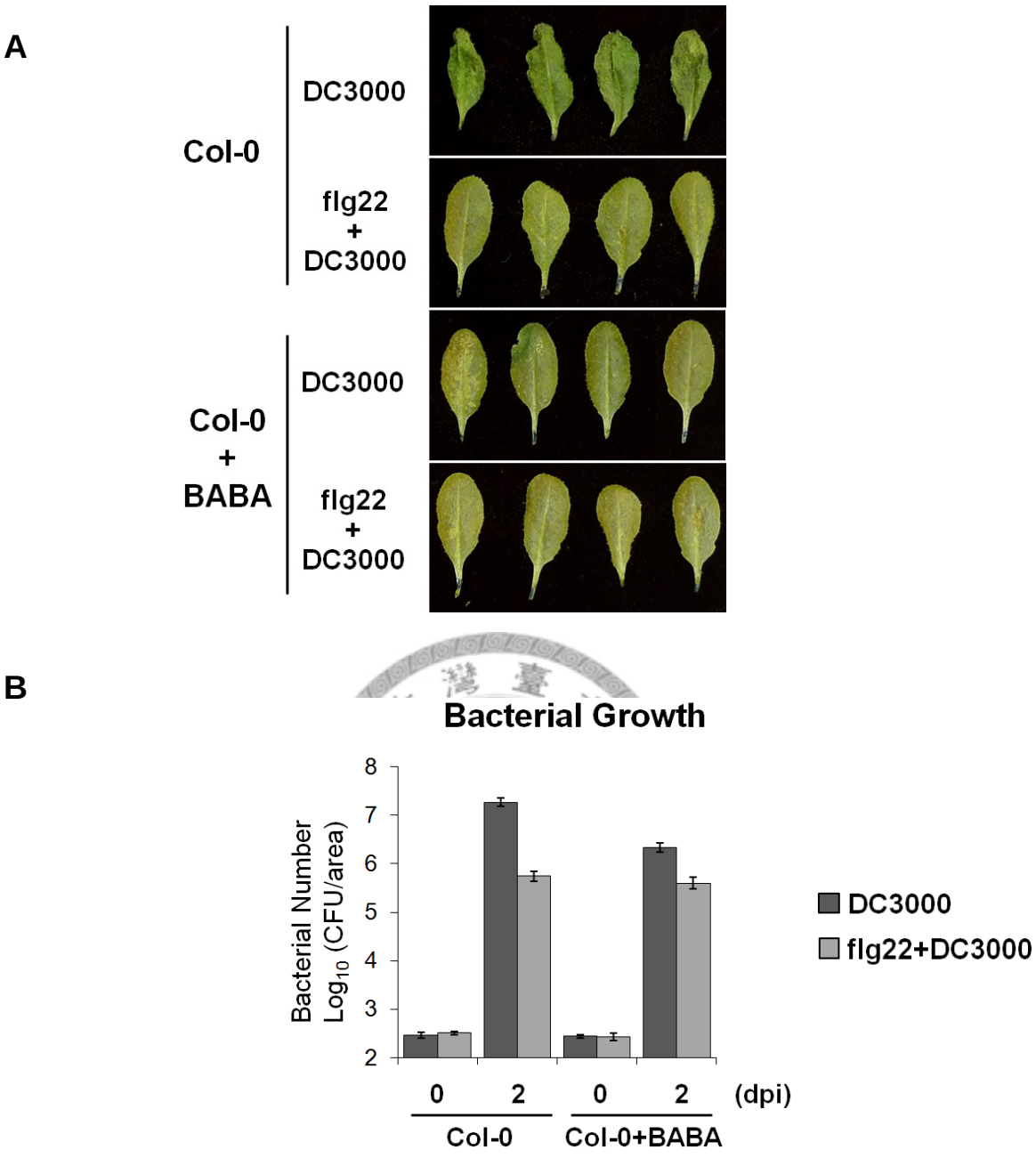

Figure 4. BABA pretreatment does not change flg22-induced resistance. **A**, Disease symptoms 4 days after *Pst* DC3000 infection. Wild-type Col-0 were pretreated for 48 h with 225 μM BABA or water and subsequently for 24 h with 1 μM flg22 or 10 mM $MgSO_4$. Plants were then infiltrated with 10^5 c.f.u. ml^{-1} *Pst* DC3000. **B**, Bacterial growth was assessed 2 days after infection. Representative results were shown, with SD of three technical replicates.

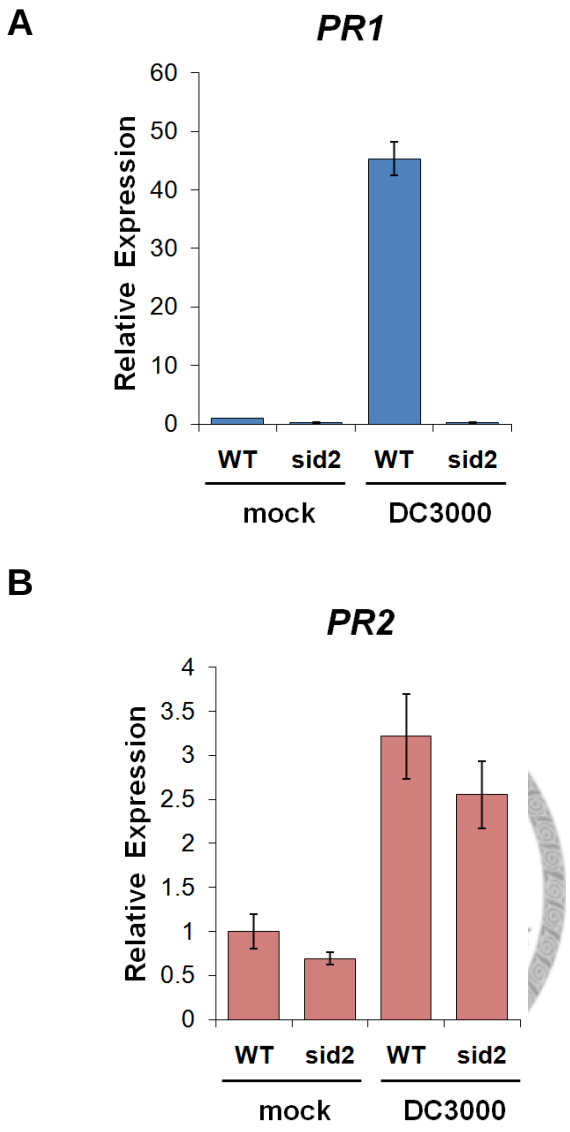

Figure 5. *PR1* expression is highly dependent on SA biosynthesis. And *PR2* expression exhibits less dependency. **A**, *PR1* expression in response to in response to dip-inoculation of 2×10^7 c.f.u. ml^{-1} *Pst* DC3000 for 18 h. **B**, *PR2* expression in response to in response to dip-inoculation of 2×10^7 c.f.u. ml^{-1} *Pst* DC3000 for 24 h. Mock controls were dipped with $MgSO_4$ only. The relative expression (in fold) is shown, with the *gene*/*EF1* values in mock WT plants as 1. Representative results were shown, with SD of three technical replicates. Similar results were obtained in at least two other independent experiments.

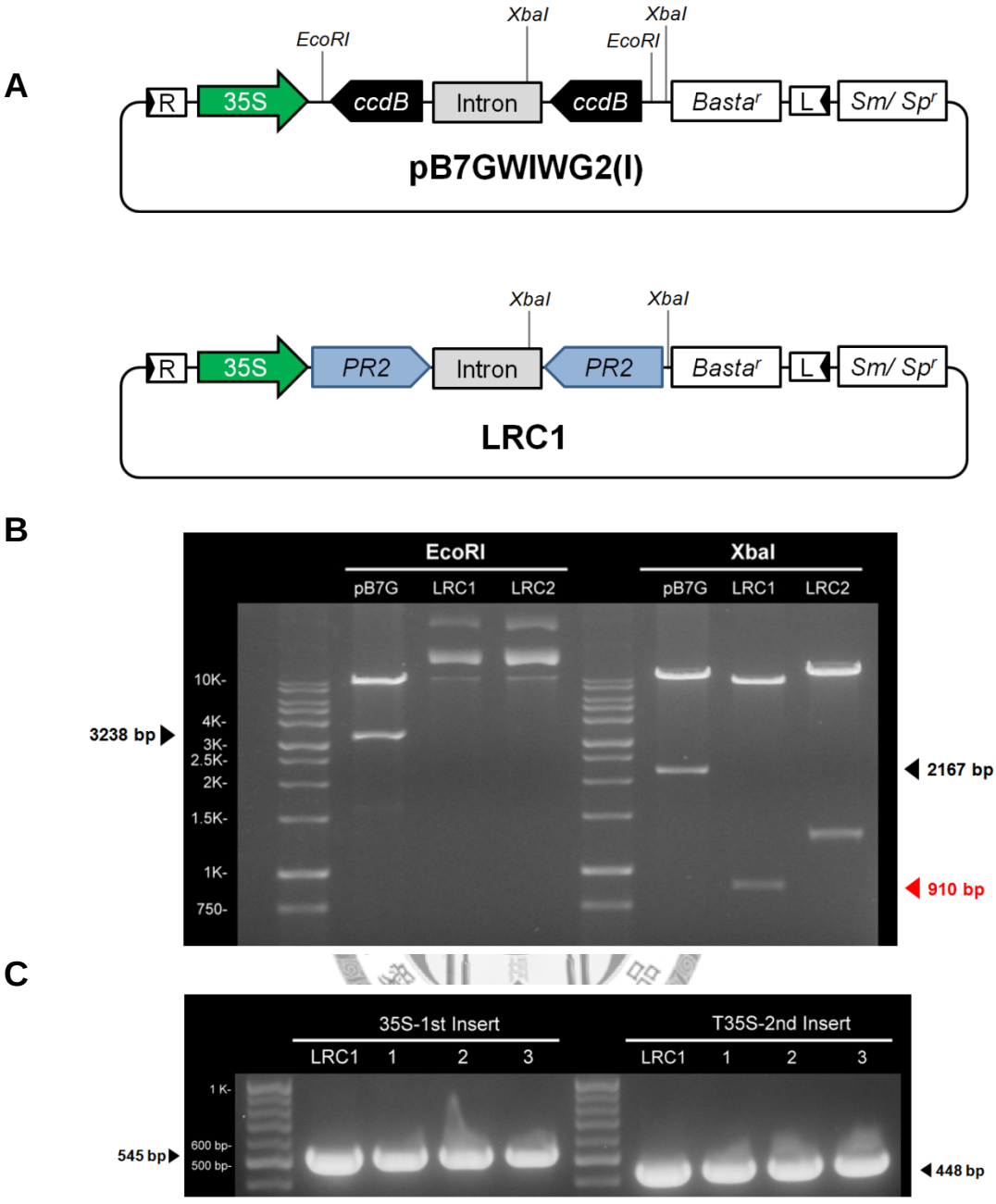

Figure 6. Outline of the map of RNAi construct for *PR2* gene silensing and confirmation of construct by restriction enzyme digestion and PCR. **A**, pB7GWIWG2(I) is the destination vector for gene silencing construct. LRC1 over-expresses inverted repeat of *PR2* fragments separated by an intron spacer. **B**, Incorporation of *PR2* fragments into pB7GWIWG2(I) were confirmed by digestion of restriction enzyme, EcoRI and XbaI. **C**, *A. tumefaciens* transformed with LRC1 were identified with 2 sets of PCR. One uses 35S promoter-specific and *PR2*-specific primer; the other uses 35S terminator-specific and *PR2*-specific primer. Different *A. tumefaciens* colonies were designated with numbers. LRC1 was positive control.

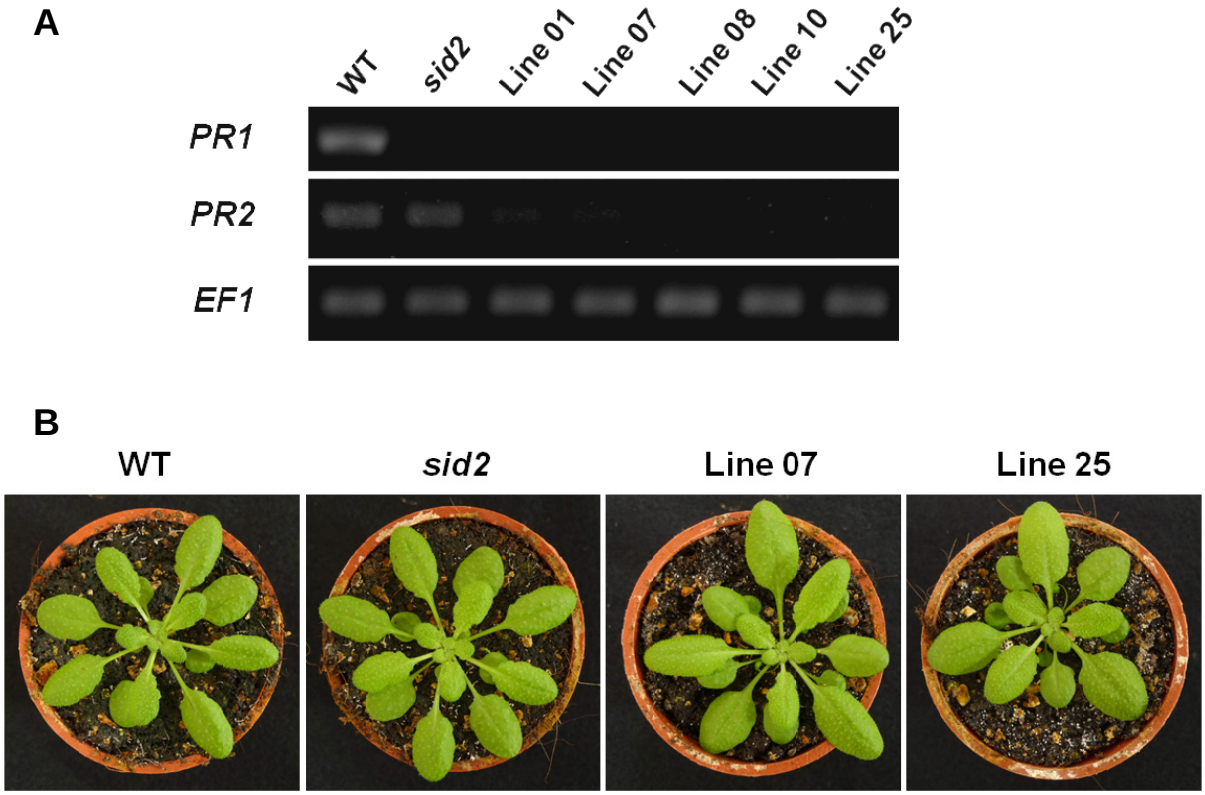

Figure 7. Transgenic plants are knock-down of *PR2* expressions. **A**, semiquantitative RT-PCR for wild-type Col-0, *sid2*, and transgenic plants in *sid2* background after dip-inoculation of 2×10^7 c.f.u. ml^{-1} *Pst* DC3000 for 24 h. **B**, Five-week-old wild-type Col-0, *sid2*, and transgenic plants line 7, 25 in *sid2* background.

A

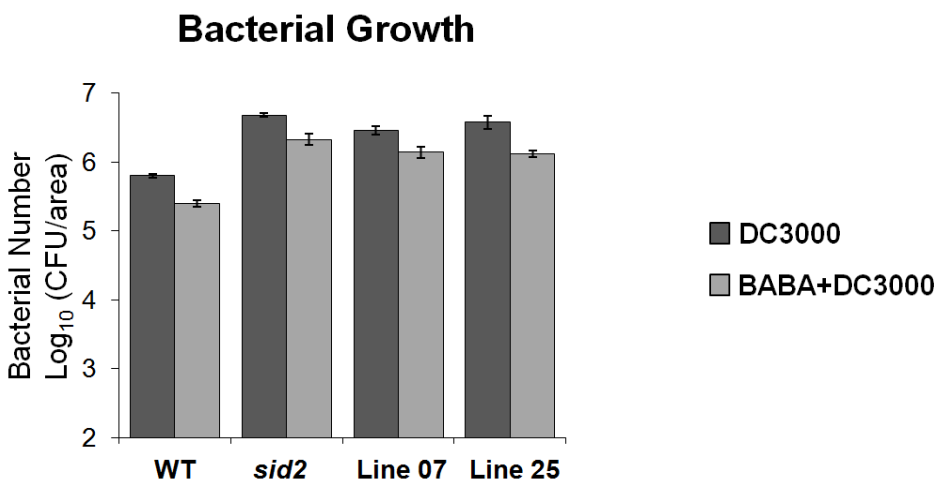

B

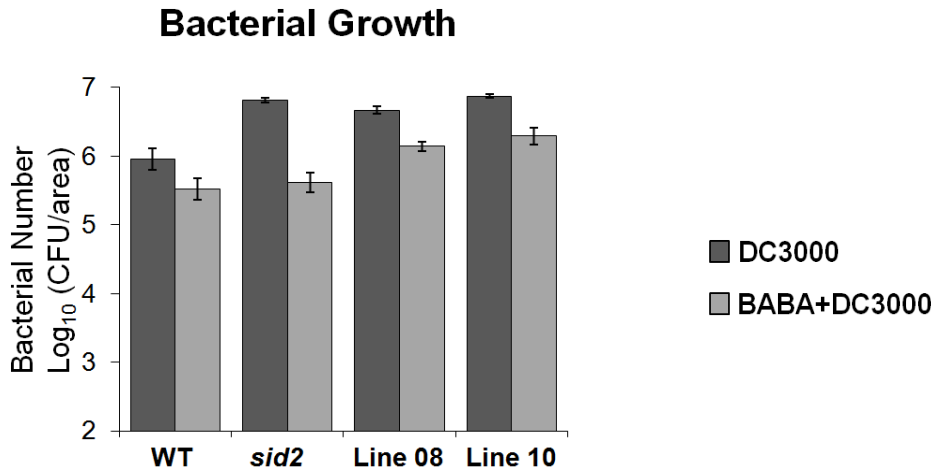

Figure 8. Bacterial growth assays for *PR2* gene silencing transgenic lines. **A** and **B**, Bacterial growth assays 2 days after dip-inoculation of 5×10^6 c.f.u. ml^{-1} *Pst* DC3000. Representative results were shown, with SD of three technical replicates.

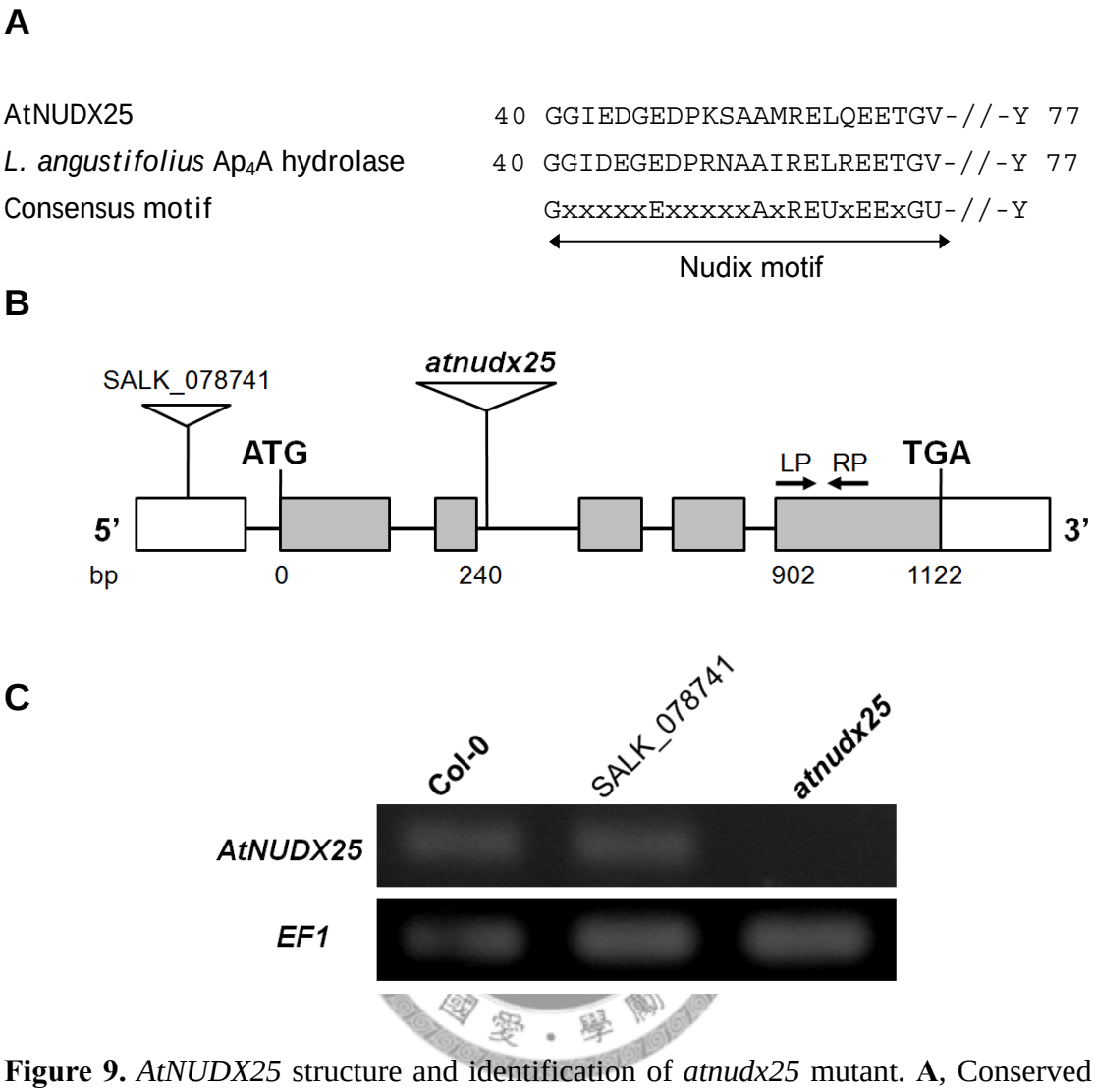

Figure 9. *AtNUDX25* structure and identification of *atnudx25* mutant. **A**, Conserved Nudix motif and downstream Tyr residue in AtNUDX25 and *L. angustifolius* Ap_4A hydrolase. **B**, Genomic structure of *AtNUDX25*. T-DNA inserted locations are indicated. Grey box, exon; thin line, intron; white box, UTR. **C**, Knock out of *AtNUDX25* transcript was examined by semiquantitative RT-PCR. The primer pair, LP and RP, is shown in (**B**).

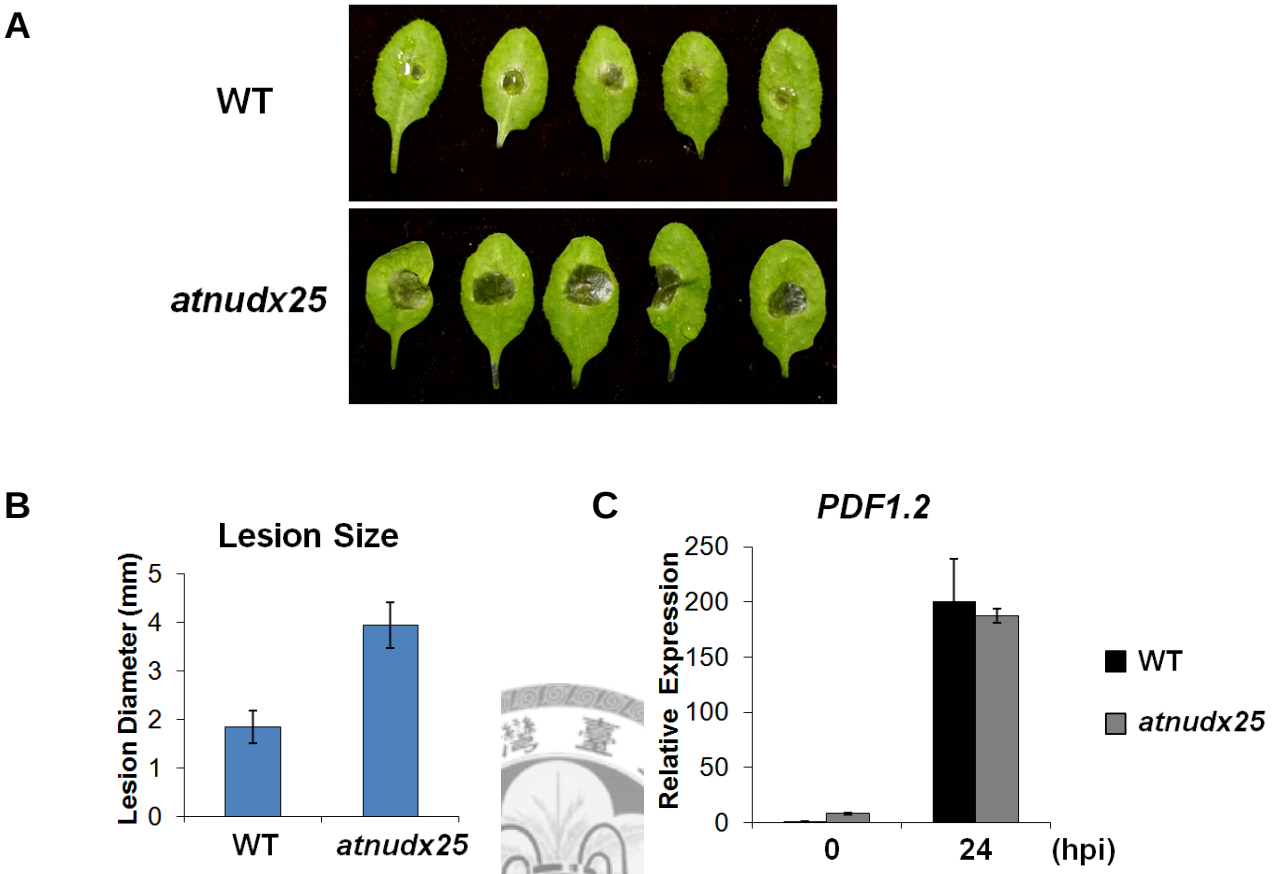

Figure 10. The *atnudx25* mutant is more susceptible to fungal pathogen *B. cinerea*. **A**, Disease symptoms 3 days after *B. cinerea* infection. Wild-type Col-0 and *atnudx25* mutant were drop-inoculated with fungal suspension of 10^5 spores ml^{-1} on leaves surface. **B**, Disease lesion size of *B. cinerea* infected leaves. Representative results were shown. Values presented are the average ± SE from at least 30 leaves measured 3 days after inoculation. **C**, *PDF1*.2 expression in response to *B. cinerea*. Samples were collected at indicated time points. The relative expression (in fold) is shown, with the *gene*/*EF1* values at 0 hpi in WT plants as 1. Representative results were shown, with SD of three technical replicates. Similar results were obtained in two other independent experiments.

Figure 11. The *atnudx25* mutant is more susceptible to bacterial pathogen *E. carotonova*. Disease symptoms 3 days after *Ecc* WPP14 infection. Wild-type Col-0 and *atnudx25* mutant were dip-inoculated with bacterial suspension of 3×10^5 c.f.u. ml^{-1}. Similar results were observed more than three times.

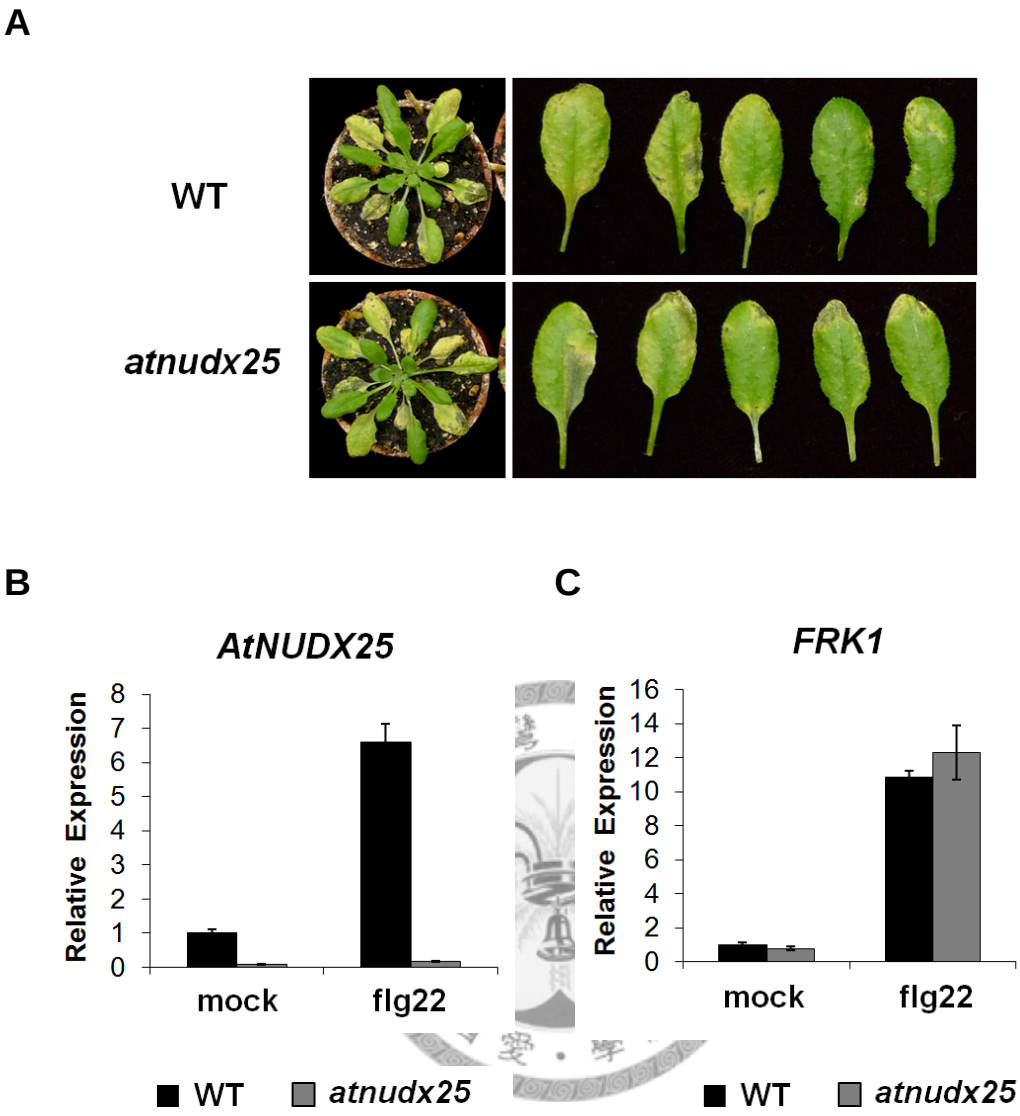

Figure 12. The *atnudx25* mutant responses normally to bacterial pathogen *P. syringae* and bacterial PAMP flg22. **A**, Disease symptoms 3 days after *Pst* DC3000 infection. Wild-type Col-0 and *atnudx25* mutant were dip-inoculated with bacterial suspension of 5×10^6 c.f.u. ml^{-1}. **B** and **C**, *AtNUDX25* and *FRK1* expression in response to 100 nM flg22. Samples were collected 1 hpi of flg22. Mock controls were infiltrated with $MgSO_4$ buffer. The relative expression (in fold) is shown, with the *gene*/*EF1* values in WT mock as 1. Results shown are the average ± SD of three technical replicates.

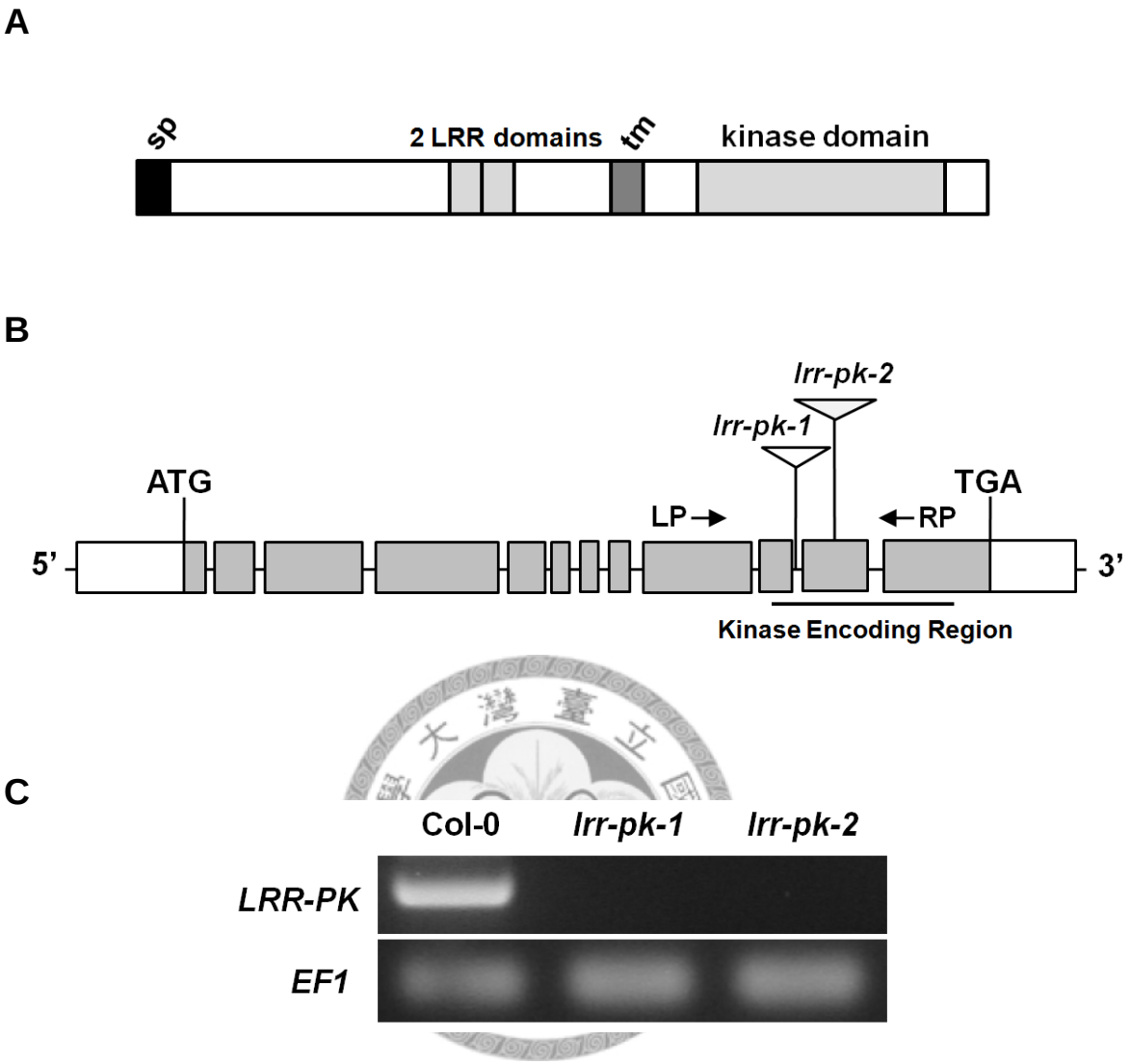

Figure 13. The putative *LRR-PK* organization and Identification of *lrr-pk* mutants. **A**, Predicted protein structure of the putative LRR-PK. Block box (sp), signal peptide; Dark grey box (tm), transmembrane domain **B**, Genomic structure of the putative *LRR-PK*. T-DNA inserted locations are indicated. Grey box, exon; thin line, intron; white box, UTR. **C**, Knock-outs of *LRR-PK* transcript were examined by semiquantitative RT-PCR. The primer pair, LP and RP, is shown in (**B**).

A

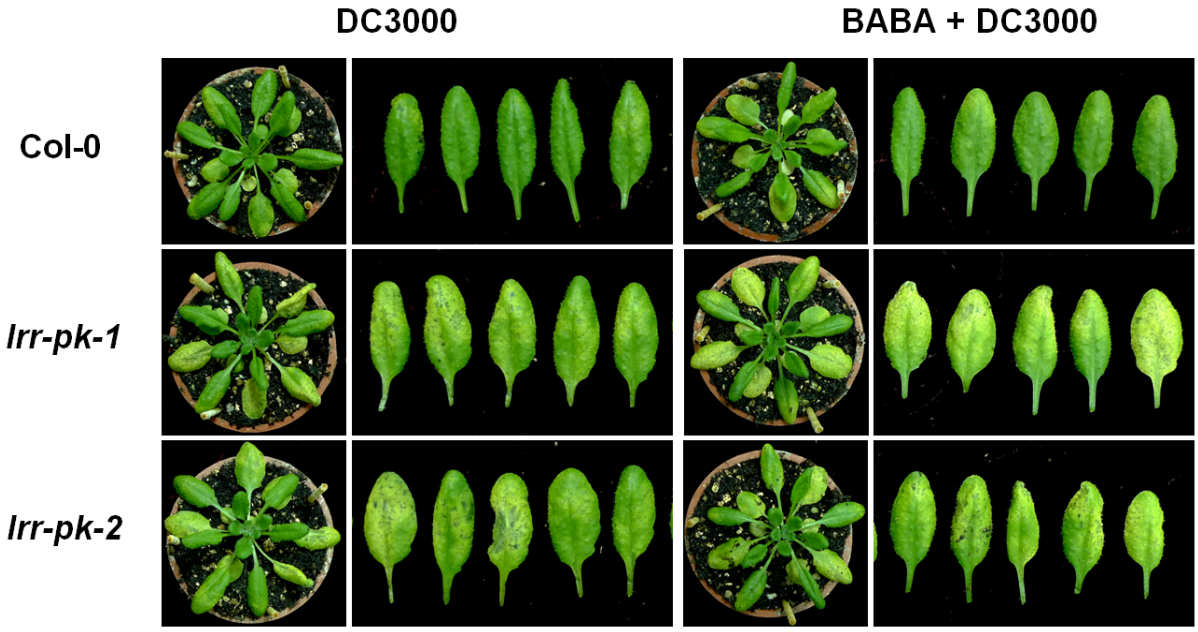
DC3000
BABA + DC3000
Col-0
lrr-pk-1
lrr-pk-2

B

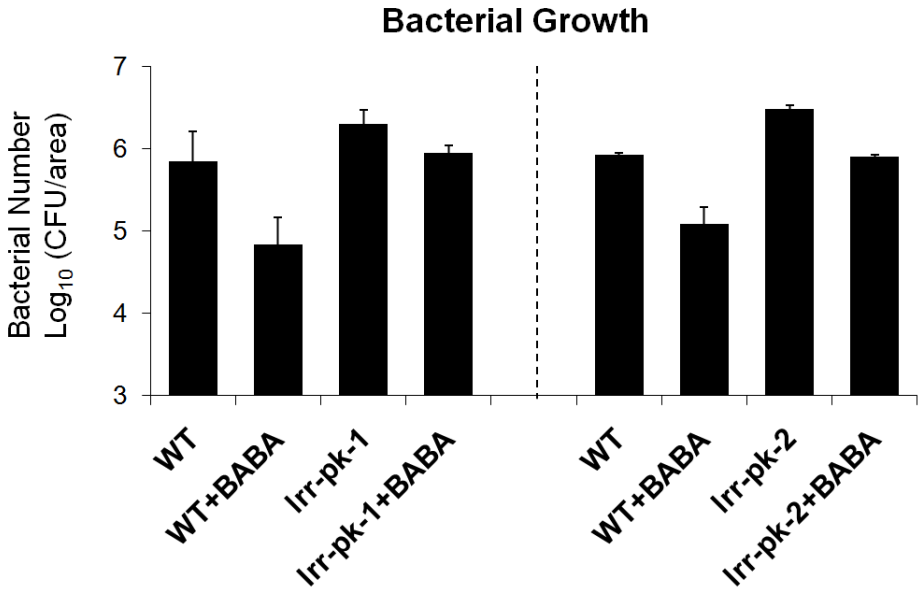
Bacterial Growth
Bacterial Number
Log10 (CFU/area)
7
6
5
4
3
WT
WT+BABA
lrr-pk-1
lrr-pk-1+BABA
WT
WT+BABA
lrr-pk-2
lrr-pk-2+BABA

C

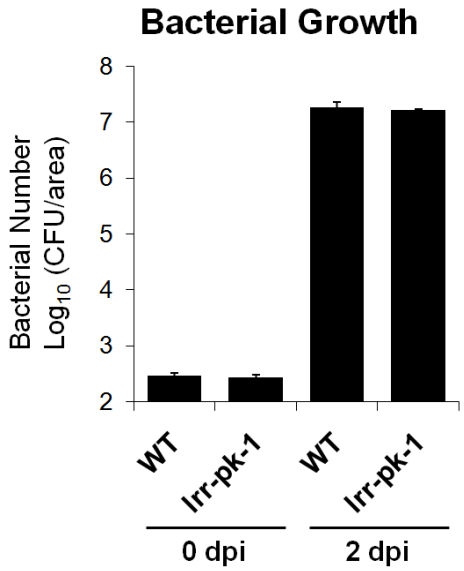

Figure 14. Mutation in the putative *LRR-PK* causes BABA partial insensitivity and enhanced susceptibility to *Pst* DC3000. **A**, Disease symptoms 3 days after *Pst* DC3000 infection. Five-week-old wild-type Col-0 and *lrr-pk-1* and *lrr-pk-2* mutants were pretreated for 48 h with 225 μM BABA or water control. Subsequently, plants were dip-inoculated with 5×10^6 c.f.u. ml^{-1} bacterial suspension. **B**, Bacterial growth assays 2 days after dip-inoculation of *Pst* DC3000. **C**, Bacterial growth assays 2 days after infiltration-inoculation with 10^5 c.f.u. ml^{-1} *Pst* DC3000. Representative results were shown, with SD of three technical replicates.

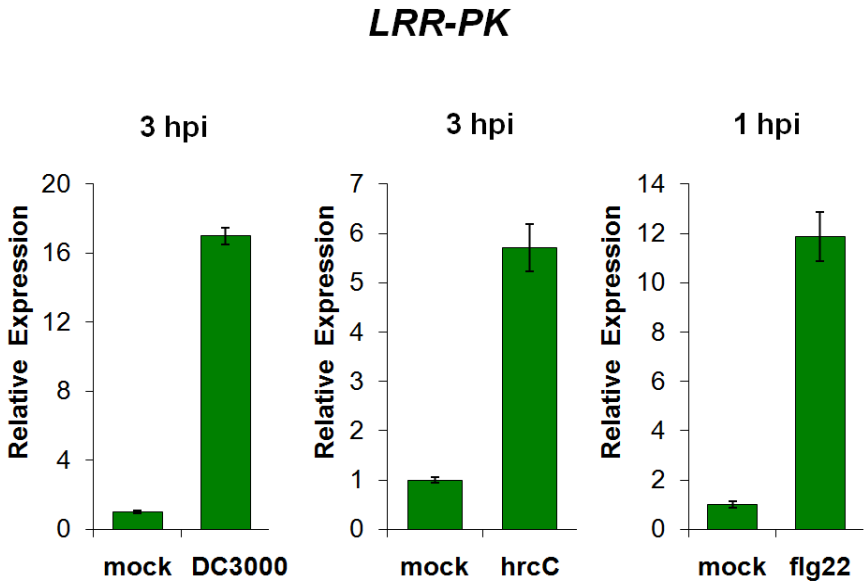

Figure 15. The putative *LRR-PK* is induced in response to bacterial infection and PAMP perception. Wild-type Col-0 were either dip-inoculated with 2×10^7 c.f.u. ml^{-1} *Pst* DC3000, or infiltrated with 10^7 c.f.u. ml^{-1} *Pst* DC3000 *hrcC*, or infiltrated with 100 nM flg22. Samples were collected at indicated time points. Mock control for infiltration is treated with $MgSO_4$ buffer. The relative expression (in fold) is shown, with the *gene*/*EF1* values in mock as 1. Results shown are the average ± SD of three technical replicates.

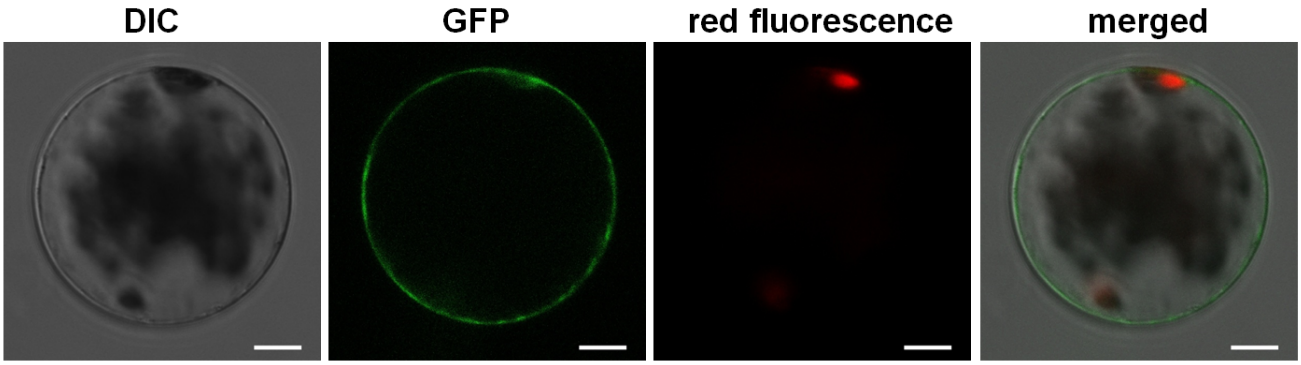

Figure 16. The putative LRR-PK localizes to the plasma membrane. Wild-type protoplast is transformed with S1G51800HGF (Gou et al., 2010) to transiently express the putative LRR-PK fused with GFP. The fluorescence was observed with confocal fluorescence microscope. White bars equals to 10 μm.

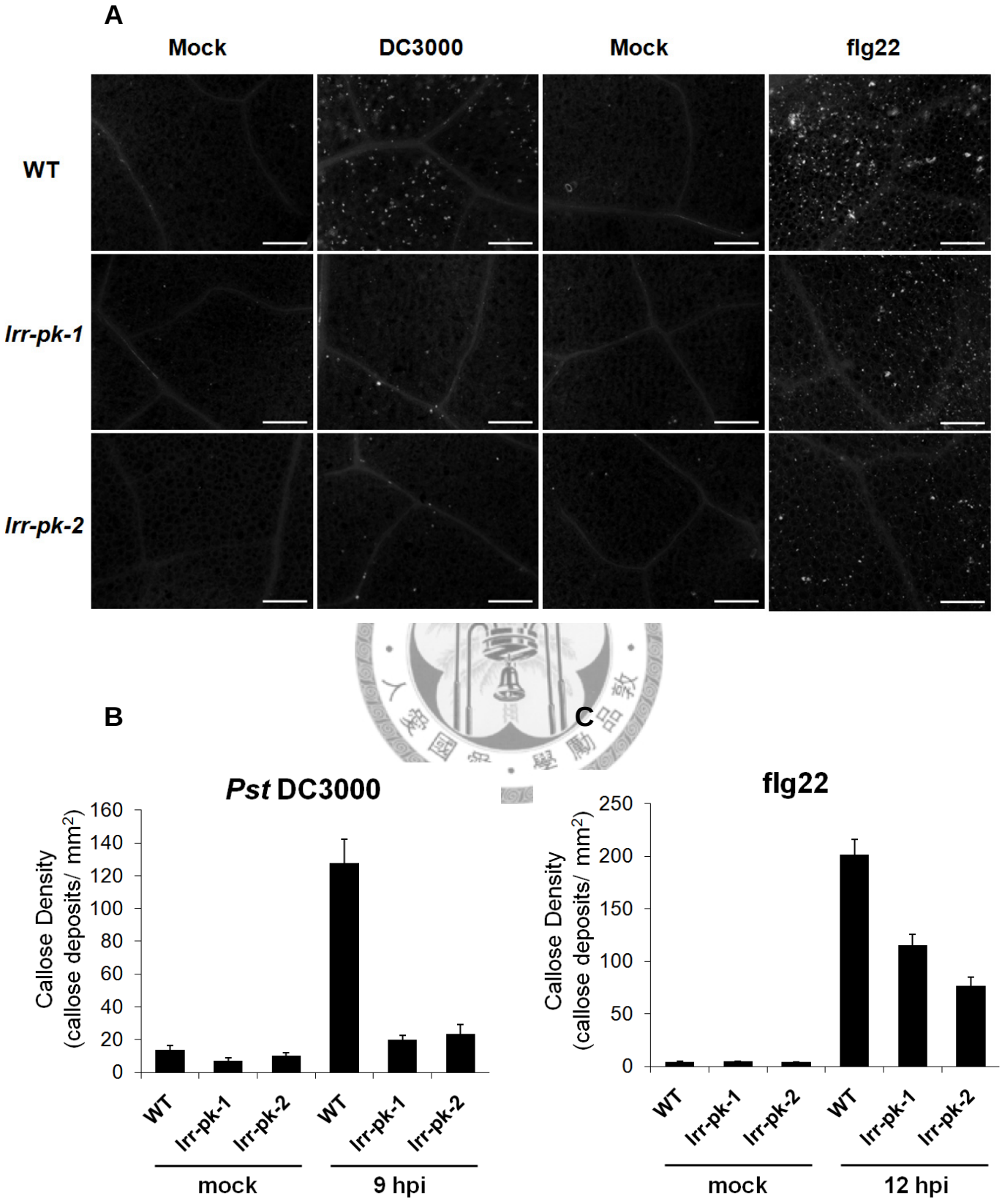
A
Mock
DC3000
Mock
flg22
WT
lrr-pk-1
lrr-pk-2
B
Pst DC3000
Callose Density
(callose deposits/ mm2)
160
140
120
100
80
60
40
20
0
WT
lrr-pk-1
lrr-pk-2
WT
lrr-pk-1
lrr-pk-2
mock
9 hpi
C
flg22
Callose Density
(callose deposits/ mm2)
250
200
150
100
50
0
WT
lrr-pk-1
lrr-pk-2
WT
lrr-pk-1
lrr-pk-2
mock
12 hpi

Figure 17. Mutation in the putative *LRR-PK* reduces callose deposition during *Pst* DC3000 infection and flg22 treatment. **A**, Col-0 wild type and *lrr-pk-1* and *lrr-pk-2* mutants were infiltrated with 10^7 c.f.u. ml^{-1} *Pst* DC3000 or 1 μM flg22. Mock controls were infiltrated with $MgSO_4$ buffer. Samples were collected at indicated time points. White bars equals to 200 μm. **B** and **C**, Measurement of callose deposition in response to *Pst* DC3000 or flg22 inoculation. Representative results were shown, with SE of at least 18 measurements. This experiment was repeated, and similar results were obtained.

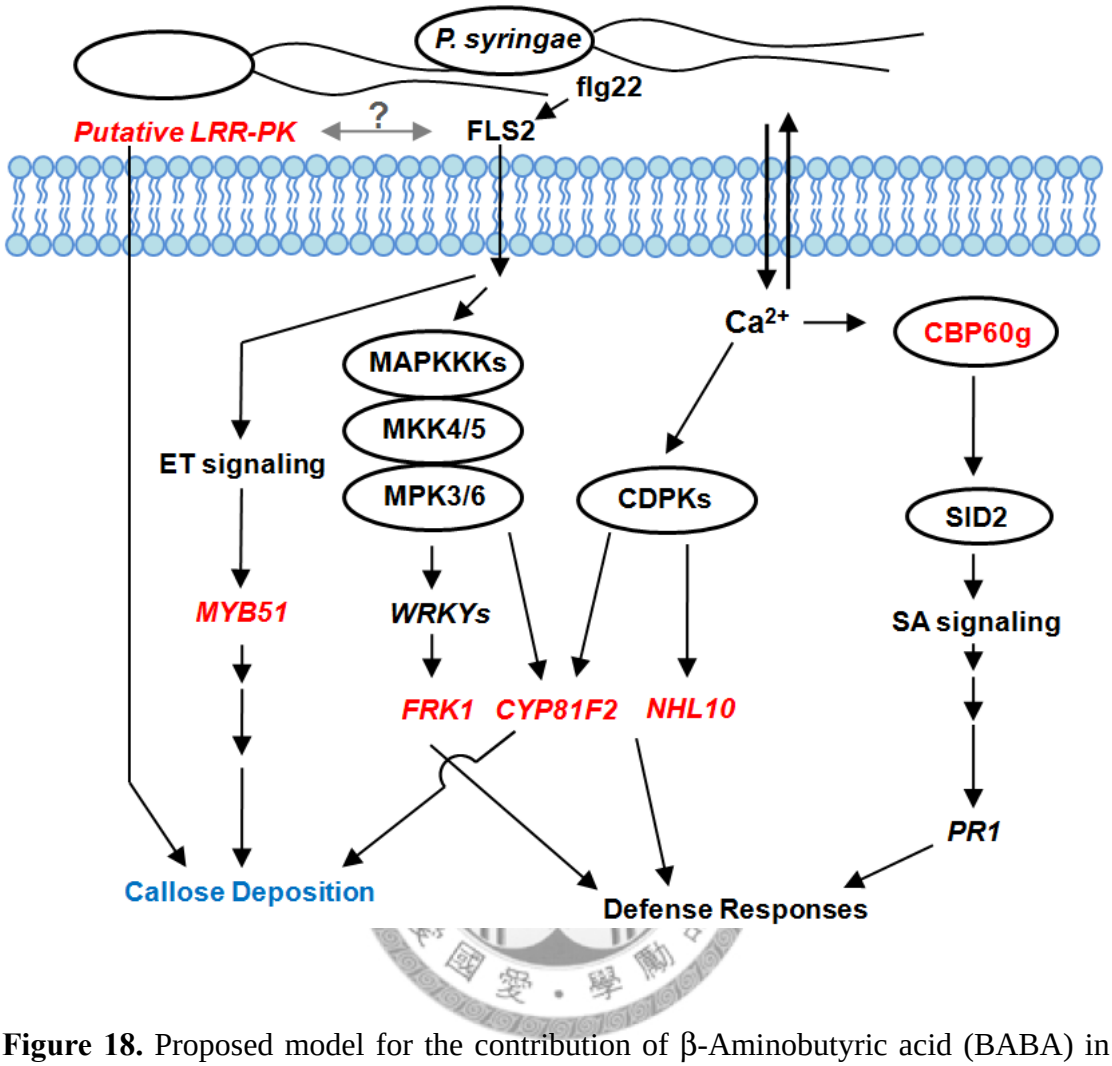

Figure 18. Proposed model for the contribution of β-Aminobutyric acid (BABA) in PAMPs-triggered defenses. Genes positively regulated by BABA pretreatment was colored red. Callose deposition up-regulated by BABA pretreatment was colored blue. The interaction between PTI and the putative LRR-PK was still unclear, hence a gray line representing their relationship was used.

Tables

Table 1. Primers for Real-Time and semi-quantitative RT-PCR

Gene		Sequence
EF1	LP	TGAGCACGCTCTTCTTGCTTTCA
(AT5G60390)	RP	GGTGGTGGCATCCATCTTGTTACA
FRK1	LP	GCCAACGGAGACATTAGAG
(AT2G19190)	RP	CCATAACGACCTGACTCATC
WRKY53	LP	CACCAGAGTCAAACCAGCCATTAC
(AT4G23810)	RP	CTTTACCATCATCAAGCCCATCGG
CYP81F2	LP	AAATGGAGAGAGCAACACAATG
*(*AT5G57220*)*	RP	ATCGCCCATTCCAATGTTAC
NHL10	LP	TTCCTGTCCGTAACCCAAAC
(AT2G35980***)***	RP	CCCTCGTAGTAGGCATGAGC
CBP60g	LP	AAGCTGGAATGTTCGATGTTC
(AT5G26920)	RP	CGTGCAACGCAAGAAACC
MYB51	LP	ACAAATGGTCTGCTATAGCT
(AT1G18570)	RP	CTTGTGTGTAACTGGATCAA
PR1	LP	AAAACTTAGCCTGGGGTAGCGG
(AT2G14610**)**	RP	CCACCATTGTTACACCTCACTTTG
PR2	LP	TGCAGAACATCGAGAACG
(AT3G57260**)**	RP	TACTCATCCCTGAACCTTCC
ATNUDX25	LP	TTTAGTGAGACTGAGGAACG
(AT3G10620)	RP	CTACCACTTCTTCTGGCTTC
LRR-PK	LP	GTTCGCCTAGAGAAACTAGC
(AT3G21340)	RP	TTTGTTGCTGAAACTGAGTC

Table 2. Primers for identifying homozygous T-DNA mutant lines.

Mutant Line		Sequence
atnudx25	LP	ACAATGAGCCACATTCTTTGC
(Salk_00093)	RP	GTTATCGTCCCAATGTTGGTG
lrr-pk-1	LP	CATCACTTTTCTCGGTCAACC
(Salk_000388)	RP	GCGGTAAAGATGCTCACTGAG
lrr-pk-2	LP	TGCGGTAAAGATGCTCACTG
(CS000992)	RP	TCATGTCTATCACGGGTTGG

Table 3. Primers for *PR2* fragment of RNAi Construct (sequence underlined, *attB* sites for Gateway recombination).

Primer	Sequence
LP	5’- GGGGACAAGTTTGTACAAAAAAGCAGGCTGACGTTGTGGCTCTTTACAA-3’
RP	5’- GGGGACCACTTTGTACAAGAAAGCTGGGTCATACTCATCCCTGAACCTTCC-3’

References

Adams-Phillips, L., Briggs, A.G., and Bent, A.F. (2010). Disruption of Poly(ADP-ribosyl)ation Mechanisms Alters Responses of Arabidopsis to Biotic Stress. Plant Physiol. **152,** 267-280.

Apel, K., and Hirt, H. (2004). REACTIVE OXYGEN SPECIES: Metabolism, Oxidative Stress, and Signal Transduction. Annu. Rev. Plant Biol. **55,** 373-399.

Asai, T., Tena, G., Plotnikova, J., Willmann, M.R., Chiu, W.-L., Gomez-Gomez, L., Boller, T., Ausubel, F.M., and Sheen, J. (2002). MAP kinase signalling cascade in Arabidopsis innate immunity. Nature **415,** 977-983.

Beckers, G.J.M., Jaskiewicz, M., Liu, Y., Underwood, W.R., He, S.Y., Zhang, S., and Conrath, U. (2009). Mitogen-Activated Protein Kinases 3 and 6 Are Required for Full Priming of Stress Responses in Arabidopsis thaliana. Plant Cell **21,** 944-953.

Boller, T., and Felix, G. (2009). A Renaissance of Elicitors: Perception of Microbe-Associated Molecular Patterns and Danger Signals by Pattern-Recognition Receptors. Annu. Rev. Plant Biol. **60,** 379-406.

Bonner, C.A., and Jensen, R.A. (1997). Recognition of specific patterns of amino acid inhibition of growth in higher plants, uncomplicated by glutamine-reversible general amino acid inhibition. Plant Sci. **130,** 133-143.

Bonner, C.A., Williams, D.S., Aldrich, H.C., and Jensen, R.A. (1996). Antagonism by L-glutamine of toxicity and growth inhibition caused by other amino acids in suspension cultures of Nicotiana silvestris. Plant Sci. **113,** 43-58.

Boudsocq, M., Willmann, M.R., McCormack, M., Lee, H., Shan, L., He, P., Bush, J., Cheng, S.-H., and Sheen, J. (2010). Differential innate immune signalling via Ca^{2+} sensor protein kinases. Nature **464,** 418-422.

Chinchilla, D., Bauer, Z., Regenass, M., Boller, T., and Felix, G. (2006). The Arabidopsis Receptor Kinase FLS2 Binds flg22 and Determines the Specificity of Flagellin Perception. Plant Cell **18,** 465-476.

Chinchilla, D., Zipfel, C., Robatzek, S., Kemmerling, B., Nurnberger, T., Jones, J.D.G., Felix, G., and Boller, T. (2007). A flagellin-induced complex of the receptor FLS2 and BAK1 initiates plant defence. Nature **448,** 497-500.

Clay, N.K., Adio, A.M., Denoux, C., Jander, G., and Ausubel, F.M. (2009). Glucosinolate Metabolites Required for an Arabidopsis Innate Immune Response. Science **323,** 95-101.

Dardick, C., and Ronald, P. (2006). Plant and Animal Pathogen Recognition

Receptors Signal through Non-RD Kinases. PLoS Pathog. **2,** e2.

Dunn, C.A., O'Handley, S.F., Frick, D.N., and Bessman, M.J. (1999). Studies on the ADP-ribose Pyrophosphatase Subfamily of the Nudix Hydrolases and Tentative Identification of trgB, a Gene Associated with Tellurite Resistance. J. Biol. Chem. **274,** 32318-32324.

Dunning, F.M., Sun, W., Jansen, K.L., Helft, L., and Bent, A.F. (2007). Identification and Mutational Analysis of Arabidopsis FLS2 Leucine-Rich Repeat Domain Residues That Contribute to Flagellin Perception. Plant Cell **19,** 3297-3313.

Durrant, W.E., and Dong, X. (2004). SYSTEMIC ACQUIRED RESISTANCE. Annu. Rev. Phytopathol. **42,** 185-209.

Edwards, K., Johnstone, C., and Thompson, C. (1991). A simple and rapid method for the preparation of plant genomic DNA for PCR analysis. Nucleic Acids Res. **19,** 1349.

Eulgem, T., and Somssich, I.E. (2007). Networks of WRKY transcription factors in defense signaling. Curr. Opin. Plant Biol. **10,** 366-371.

Felix, G., Duran, J.D., Volko, S., and Boller, T. (1999). Plants have a sensitive perception system for the most conserved domain of bacterial flagellin. Plant J. **18,** 265-276.

Finn, R.D., Mistry, J., Tate, J., Coggill, P., Heger, A., Pollington, J.E., Gavin, O.L., Gunasekaran, P., Ceric, G., Forslund, K., Holm, L., Sonnhammer, E.L.L., Eddy, S.R., and Bateman, A. (2010). The Pfam protein families database. Nucleic Acids Res. **38,** D211-222.

Flors, V., Ton, J., Doorn, R.v., Jakab, G., García-Agustín, P., and Mauch-Mani, B. (2008). Interplay between JA, SA and ABA signalling during basal and induced resistance against *Pseudomonas syringae* and *Alternaria brassicicola*. Plant J. **54,** 81-92.

Gómez-Gómez, L., and Boller, T. (2000). FLS2: An LRR Receptor-like Kinase Involved in the Perception of the Bacterial Elicitor Flagellin in Arabidopsis. Mol. Cell **5,** 1003-1011.

Gómez-Gómez, L., Felix, G., and Boller, T. (1999). A single locus determines sensitivity to bacterial flagellin in Arabidopsis thaliana. Plant J. **18,** 277-284.

Ge, X., Li, G.-J., Wang, S.-B., Zhu, H., Zhu, T., Wang, X., and Xia, Y. (2007). AtNUDT7, a Negative Regulator of Basal Immunity in Arabidopsis, Modulates Two Distinct Defense Response Pathways and Is Involved in Maintaining Redox Homeostasis. Plant Physiol. **145,** 204-215.

Glazebrook, J. (2005). Contrasting Mechanisms of Defense Against Biotrophic and Necrotrophic Pathogens. Annu. Rev. Phytopathol. **43,** 205-227.

Goerlich, O., Foeckler, R., and Holler, E. (1982). Mechanism of Synthesis of Adenosine(5')tetraphospho(5')adenosine (AppppA) by Aminoacyl-tRNA Synthetases. Eur. J. Biochem. **126,** 135-142.

Gou, X., He, K., Yang, H., Yuan, T., Lin, H., Clouse, S., and Li, J. (2010). Genome-wide cloning and sequence analysis of leucine-rich repeat receptor-like protein kinase genes in Arabidopsis thaliana. BMC Genomics **11,** 19.

Guranowski, A., Brown, P., Ashton, P.A., and Blackburn, G.M. (1994). Regiospecificity of the hydrolysis of diadenosine polyphosphates catalyzed by three specific pyrophosphohydrolases. Biochemistry **33,** 235-240.

Hahlbrock, K., and Scheel, D. (1989). Physiology and Molecular Biology of Phenylpropanoid Metabolism. Annu. Rev. Plant Physiol. Plant Mol. Biol. **40,** 347-369.

Ham, J.H., Kim, M.G., Lee, S.Y., and Mackey, D. (2007). Layered basal defenses underlie non-host resistance of Arabidopsis to *Pseudomonas syringae* pv. *phaseolicola*. Plant J. **51,** 604-616.

Jakab, G., Ton, J., Flors, V., Zimmerli, L., Metraux, J.-P., and Mauch-Mani, B. (2005). Enhancing Arabidopsis Salt and Drought Stress Tolerance by Chemical Priming for Its Abscisic Acid Responses. Plant Physiol. **139,** 267-274.

Jambunathan, N., and Mahalingam, R. (2006). Analysis of Arabidopsis *Growth Factor Gene 1* (*GFG1*) encoding a nudix hydrolase during oxidative signaling. Planta **224,** 1-11.

Kohler, A., Schwindling, S., and Conrath, U. (2002). Benzothiadiazole-Induced Priming for Potentiated Responses to Pathogen Infection, Wounding, and Infiltration of Water into Leaves Requires the *NPR1/NIM1* Gene in Arabidopsis. Plant Physiol. **128,** 1046-1056.

Kunze, G., Zipfel, C., Robatzek, S., Niehaus, K., Boller, T., and Felix, G. (2004). The N Terminus of Bacterial Elongation Factor Tu Elicits Innate Immunity in Arabidopsis Plants. Plant Cell **16,** 3496-3507.

Lee, P.C., Bochner, B.R., and Ames, B.N. (1983). AppppA, heat-shock stress, and cell oxidation. Proc. Natl. Acad. Sci. USA **80,** 7496-7500.

Melotto, M., Underwood, W., Koczan, J., Nomura, K., and He, S.Y. (2006). Plant Stomata Function in Innate Immunity against Bacterial Invasion. Cell **126,** 969-980.

Millet, Y.A., Danna, C.H., Clay, N.K., Songnuan, W., Simon, M.D., Werck-Reichhart, D., and Ausubel, F.M. (2010). Innate Immune Responses Activated in Arabidopsis Roots by Microbe-Associated Molecular Patterns.

Plant Cell **22,** 973-990.

Nawrath, C., and Metraux, J.-P. (1999). Salicylic Acid Induction–Deficient Mutants of Arabidopsis Express *PR-2* and *PR-5* and Accumulate High Levels of Camalexin after Pathogen Inoculation. Plant Cell **11,** 1393-1404.

Nicaise, V., Roux, M., and Zipfel, C. (2009). Recent Advances in PAMP-Triggered Immunity against Bacteria: Pattern Recognition Receptors Watch over and Raise the Alarm. Plant Physiol. **150,** 1638-1647.

Ogawa, T., Ueda, Y., Yoshimura, K., and Shigeoka, S. (2005). Comprehensive Analysis of Cytosolic Nudix Hydrolases in Arabidopsis thaliana. J. Biol. Chem. **280,** 25277-25283.

Ogawa, T., Yoshimura, K., Miyake, H., Ishikawa, K., Ito, D., Tanabe, N., and Shigeoka, S. (2008). Molecular Characterization of Organelle-Type Nudix Hydrolases in Arabidopsis. Plant Physiol. **148,** 1412-1424.

Robatzek, S., Bittel, P., Chinchilla, D., Köchner, P., Felix, G., Shiu, S.-H., and Boller, T. (2007). Molecular identification and characterization of the tomato flagellin receptor LeFLS2, an orthologue of Arabidopsis FLS2 exhibiting characteristically different perception specificities. Plant Mol. Biol. **64,** 539-547.

Szurmak B, W.-C.A., Wszelaka-Rylik M, Bal W, Dobrzańska M. (2008). A diadenosine 5', 5"-P^1P^4 tetraphosphate (Ap_4A) hydrolase from *Arabidopsis thaliana* that is activated preferentially by Mn^{2+} ions. Acta Biochim. Pol. **55,** 151-160.

Ton, J., and Mauch-Mani, B. (2004). Beta-amino-butyric acid-induced resistance against necrotrophic pathogens is based on ABA-dependent priming for callose. Plant J. **38,** 119-130.

Tsuda, K., Sato, M., Glazebrook, J., Cohen, J.D., and Katagiri, F. (2008). Interplay between MAMP-triggered and SA-mediated defense responses. Plant J. **53,** 763-775.

Vartanian, A., Prudovsky, I., Suzuki, H., Dal Pra, I., and Kisselev, L. (1997). Opposite effects of cell differentiation and apoptosis on Ap_3A/Ap_4A ratio in human cell cultures. FEBS Lett. **415,** 160-162.

Wang, L., Tsuda, K., Sato, M., Cohen, J.D., Katagiri, F., and Glazebrook, J. (2009). Arabidopsis CaM Binding Protein CBP60g Contributes to MAMP-Induced SA Accumulation and Is Involved in Disease Resistance against *Pseudomonas syringae*. PLoS Pathog. **5,** e1000301.

Wu, C.-C., Singh, P., Chen, M.-C., and Zimmerli, L. (2010). L-Glutamine inhibits beta-aminobutyric acid-induced stress resistance and priming in Arabidopsis. J. Exp. Bot. **61,** 995-1002.

Yannay-Cohen, N., Carmi-Levy, I., Kay, G., Yang, C.M., Han, J.M., Kemeny, D.M., Kim, S., Nechushtan, H., and Razin, E. (2009). LysRS Serves as a Key Signaling Molecule in the Immune Response by Regulating Gene Expression. Mol. Cell **34,** 603-611.

Yoo, S.-D., Cho, Y.-H., and Sheen, J. (2007). Arabidopsis mesophyll protoplasts: a versatile cell system for transient gene expression analysis. Nat. Protocols **2,** 1565-1572.

Zimmerli, L., Metraux, J.-P., and Mauch-Mani, B. (2001). Beta-Aminobutyric Acid-Induced Protection of Arabidopsis against the Necrotrophic Fungus *Botrytis cinerea*. Plant Physiol. **126,** 517-523.

Zimmerli, L., Jakab, G., Metraux, J.-P., and Mauch-Mani, B. (2000). Potentiation of pathogen-specific defense mechanisms in Arabidopsis by beta -aminobutyric acid. Proc. Natl. Acad. Sci. USA **97,** 12920-12925.

Zimmerli, L., Bi-Huei, H., Chia-Hong, T., Jakab, G., Mauch-Mani, B., and Somerville, S. (2008). The xenobiotic β-aminobutyric acid enhances Arabidopsis thermotolerance. Plant J. **53,** 144-156.

Zipfel, C., Robatzek, S., Navarro, L., Oakeley, E.J., Jones, J.D.G., Felix, G., and Boller, T. (2004). Bacterial disease resistance in Arabidopsis through flagellin perception. Nature **428,** 764-767.

Zipfel, C., Kunze, G., Chinchilla, D., Caniard, A., Jones, J.D.G., Boller, T., and Felix, G. (2006). Perception of the Bacterial PAMP EF-Tu by the Receptor EFR Restricts Agrobacterium-Mediated Transformation. Cell **125,** 749-760.